

An early Sox2-dependent gene expression program required for hippocampal dentate gyrus development

Sara Mercurio, Chiara Alberti, Linda Serra, Simone Meneghini, Jessica Bertolini, Pietro Berico, Andrea Becchetti and Silvia K. Nicolis

Department of Biotechnology and Biosciences, University of Milano-Bicocca, piazza della Scienza 2, 20126 Milano, Italy

Correspondence: silvia.nicolis@unimib.it, sara.mercurio@unimib.it

Abstract

The hippocampus is a brain area central for cognition. Mutations in the human SOX2 transcription factor cause neurodevelopmental defects, leading to intellectual disability and seizures, together with hippocampal dysplasia. We generated an allelic series of Sox2 conditional mutations in mouse, deleting Sox2 at different developmental stages. Late Sox2 deletion (from E11.5, via Nestin-Cre) affects only postnatal hippocampal development; earlier deletion (from E10.5, Emx1-Cre) significantly reduces the dentate gyrus, and the earliest deletion (from E9.5, FoxG1-Cre) causes drastic abnormalities, with almost complete absence of the dentate gyrus. We identify a set of functionally interconnected genes (Gli3, Wnt3a, Cxcr4, p73 and Tbr2), known to play essential roles in hippocampal embryogenesis, which are downregulated in early Sox2 mutants, and (Gli3 and Cxcr4) directly controlled by SOX2; their downregulation provides plausible molecular mechanisms contributing to the defect. Electrophysiological studies of the Emx1Cre mouse model reveal altered excitatory transmission in CA1 and CA3 regions.

30

31 **Introduction**

32

33 The hippocampus is a brain region important for cognition, playing essential roles in learning and
34 in spatial and episodic memory formation. Hippocampus defects (of genetic origin, or acquired) can
35 lead to intellectual disability (ID), deficits of memory formation, and epilepsy (Kandel, Schwartz,
36 & Jessell, 2000).

37 Within the hippocampus, the dentate gyrus (DG) represents the primary input site for excitatory
38 neuronal projections; the major type of DG neurons (granule neurons) are generated by neural stem
39 cells (NSC) that are defined early in development, and continue neurogenesis during embryogenesis
40 and also in postnatal stages, in mice as well as in humans (Berg et al., 2019; Zhong et al., 2020).

41

42 Patients carrying heterozygous loss-of-function mutations in the gene encoding the SOX2
43 transcription factor show a characteristic spectrum of central nervous system (CNS) defects,
44 including hippocampal defects (involving the dentate gyrus), ID, and epilepsy (Fantes et al., 2003;
45 Kondoh H, 2016; Ragge et al., 2005; Sisodiya et al., 2006). Understanding the developmental
46 events and the genetic program controlled by SOX2 during hippocampal embryogenesis therefore
47 provides a key to understand how their perturbation can lead to hippocampal disease (in SOX2-
48 mutant patients and, more in general, in hippocampal defects of genetic origin).

49

50 In mouse, Sox2-dependent hippocampal disease has been previously modelled by conditional
51 mutagenesis (Favaro et al., 2009). Sox2 pan-neural deletion at mid-embryogenesis, via a Nestin-Cre
52 transgene, led to a relatively normal hippocampal development up to birth; at early postnatal stages,
53 however, the hippocampus failed to complete its development, and remained hypoplastic, due to a
54 failure of postnatal DG NSC. The study of SOX2 binding to DNA in NSC proved instrumental in
55 the identification of various Sox2 target genes, playing important roles in the development of
56 different brain regions in vivo, such as the basal ganglia (A. Ferri et al., 2013), the cerebellum
57 (Cerrato et al., 2018), and the visual thalamus (Mercurio et al., 2019).

58

59 While postnatal hippocampal development was perturbed following Nestin-Cre-mediated Sox2
60 deletion, embryonic hippocampal development was, quite surprisingly, very little, if at all, affected
61 in these mutants (Favaro et al., 2009). In principle, this could be due to redundant functions played
62 by other homologous genes of the SoxB family, such as Sox1 and Sox3, coexpressed with Sox2 in

the developing neural tube, and reported to function in hippocampal neural stem/progenitor cells (Rogers et al., 2013); alternatively, we reasoned that Sox2 may play non-redundant, very early functions in hippocampal development, that might not be revealed by Nestin-Cre-mediated deletion.

Here, we generated an allelic series of Sox2 conditional mutations, using Cre transgenes deleting Sox2 at stages earlier than Nestin-Cre: FoxG1-Cre, active from embryonic day (E) 8.5 (Hébert & McConnell, 2000), and Emx1-Cre (Gorski et al., 2002), active from E10.5. We report that early Sox2 deletion leads to drastic defects of hippocampal development, the earlier the deletion, the stronger the phenotype: in Emx1-Cre mutants, hippocampal development is perturbed, but still present, but in FoxG1-Cre mutants, hippocampal development is severely impaired, and the DG essentially fails to develop. We propose that Sox2 sets in motion a very early gene expression program in the hippocampal primordium, required for all of its subsequent development. Indeed, we show that early (but not late) Sox2 deletion reduces the expression of several genes (some of which SOX2-bound), individually characterized by previous studies as master regulators of hippocampal development (and human neurodevelopmental disease), including Gli3, Wnt3a, Cxcr4, Tbr2 and p73, some of which are known to cross-regulate each other.

Results

Sox2 is expressed in the primordium of the developing hippocampus and in the adjacent cortical hem

The transcription factor Sox2 is expressed throughout the neural tube from the beginning of its development (Avilion et al., 2003; Favaro et al., 2009; A. L. Ferri et al., 2004; Mariani et al., 2012). The hippocampus starts to develop around embryonic day (E) 12.5, in the medial wall of the telencephalon, and becomes morphologically recognizable in the following days (Fig. 1A) (Berg et al., 2019; Hodge et al., 2012). A region essential for the formation of the hippocampus is the cortical hem (CH), also known as the hippocampal organizer, identified in mice at E12.5; signaling from the CH is able to organize the surrounding tissue into a hippocampus (Grove, 2008; Mangale et al., 2008). The dentate neural epithelium (DNE), adjacent to the cortical hem (Fig. 1A), contains neural stem cells (NSC), that will generate granule neurons in the hippocampus dentate gyrus (DG) throughout development and, subsequently, in postnatal life (Berg et al., 2019). On the outer side

96 of the neuroepithelium, towards the pia, a population of neurons, called Cajal-Retzius cells (CRC)
 97 (Fig. 1A) develops, that will have a key role in the morphogenesis of the hippocampus. NSC and
 98 intermediate neural progenitors (INP) will migrate from the DNE, along the dorsal migratory
 99 stream (DMS), towards the forming hippocampal fissure (HF), a folding of the meninges that will
 100 be invaded by CRC (Fig. 1A).

101 We examined Sox2 expression by *in situ* hybridization (ISH) and immunofluorescence (IF), in the
 102 medial telencephalon, from which the hippocampus develops, between E12.5 and E18.5 (Fig. 1B-
 103 I). At E10.5 Sox2 is expressed in the whole telencephalon including the dorso-medial region that
 104 will give rise to the hippocampus (Fig. 1B). At E12.5, Sox2 is expressed throughout the
 105 neuroepithelium in the medial telencephalic wall and it is enriched in the CH region (Fig. 1C); at
 106 E15.5, expression persists in the neuroepithelium, and is detected in the DMS and in the fimbria (a
 107 CH derivative) (Fig. 1D). Just before birth, at E18.5, Sox2 expression is detected in the developing
 108 DG (Fig. 1E,E').

109 We then performed co-immunohistochemistry experiments with antibodies against SOX2, and
 110 markers of more differentiated cell types: CR cells markers Reelin and P73 (Fig. 1F,G,I) and the
 111 pan-neuronal marker TuJ1 (Fig. 1H). While SOX2 was detected in all cells within the
 112 neuroepithelium, as expected, we detected no or very little (Fig. 1F arrowheads) overlap with TuJ1,
 113 Reelin, or p73 (Fig. 1 F-I). Moreover, to test if Sox2 is expressed in the progenitors of CRC, we
 114 turned on EYFP in Sox2-expressing cells of the early telencephalon before CRC differentiation
 115 started, at E9.5 (via a Sox2-CreERT2 transgene and a lox-stop-lox reporter of Cre activity, Fig. S1),
 116 and found that these cells differentiated into Reelin-expressing CRC in the hippocampal fissure and
 117 the cortex (Fig. S1).

118 Thus, Sox2 expression in the developing hippocampus and CH is present mainly in undifferentiated
 119 neuroepithelial cells (including CRC precursors), and becomes extinguished in differentiation.

121 ***Sox2 early ablation (FoxG1-Cre) prevents the development of the hippocampal dentate gyrus,*** 122 ***and severely compromises hippocampal embryogenesis***

123 Sox2 is required for postnatal development of the hippocampus, in particular to maintain NSC in
 124 the DG (Favaro et al., 2009); however, whether Sox2 has a role in hippocampus embryogenesis was
 125 not known. To address this question, we generated three different conditional knock-outs, to ablate
 126 Sox2 at different time points of telencephalon development. Specifically, we crossed a Sox2 floxed
 127 allele (Favaro et al., 2009) with the following Cre lines: FoxG1-Cre, deleting between E8.5 and

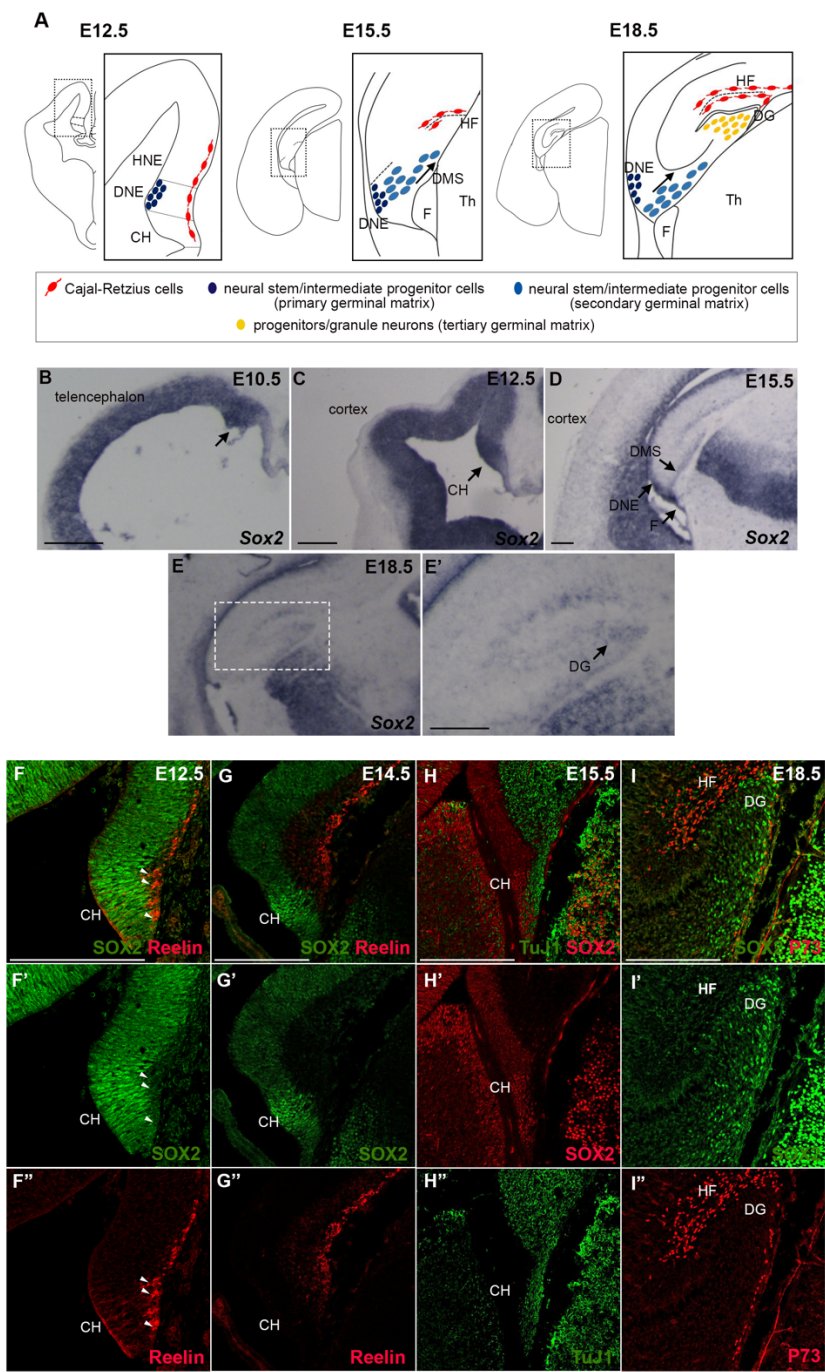


Figure 1

Sox2 expression in the dorsal telencephalon.

(A) Schematic representation of the development of the hippocampus in the dorsal telencephalon. (B-E) *In situ* hybridization for Sox2 on coronal section of mouse brains at E10.5 (B) E12.5 (C), E15.5 (D), E18.5 (E). Arrows indicate Sox2 expression in the developing hippocampus in particular in the dorsal telencephalon in (B), in the cortical hem (CH) in (C), in the dorsal migratory stream (DMS) in (D) and in the dentate gyrus (DG) in (E'). (F-I) Immunofluorescence of Sox2 (F-I), of markers of CRC, Reelin (F,G) and P73 (I), and of a marker of differentiating neurons TuJ1 (H). Representative single optical confocal sections are shown. Scale bars 200 μm. CH, cortical hem; DNE, dentate neuroepithelium; HNE, hippocampal neuroepithelium; DMS, dentate migratory stream; HF, hippocampal fissure; DG, dentate gyrus; F, fimbria; Th, thalamus.

140 E9.5 (A. Ferri et al., 2013; Hébert & McConnell, 2000), Emx1-Cre, deleting after E10.5 (Gorski et
141 al., 2002), and Nestin-Cre, deleting after E11.5 (Tronche et al., 1999). The resulting conditional
142 knock-outs (Sox2^{flox/flox};FoxG1-Cre; Sox2^{flox/flox};Emx1-Cre; Sox2^{flox/flox};Nestin-Cre) will be called
143 FoxG1-Cre cKO, Emx1-Cre cKO and Nestin-Cre cKO respectively, from now onwards. As
144 expected, complete Sox2 deletion is observed already at E9.5 in FoxG1-Cre cKO (in the whole
145 telencephalon), and at E10.5 in Emx1-Cre cKO (in the dorsal telencephalon); in the Nestin-Cre
146 cKO, deletion occurs after E11.5 (Favaro et al., 2009, Ferri et al., 2013, and data not shown).

147
148 We initially explored hippocampus development in the different mutants at the end of gestation
149 (E18.5; P0), performing ISH with probes identifying hippocampal structures and cell types (Fig. 2).
150 ISH for a general marker of the developing hippocampus, Cadherin 8 (Korematsu & Redies, 1997),
151 shows that, at the end of gestation (E18.5, P0) the DG appears little, if at all, affected in the Nestin-
152 Cre cKO (Fig. 2C), as expected (Favaro et al., 2009). However, in the Emx1-Cre cKO, the DG is
153 greatly reduced, in particular anteriorly (Fig. 2B); remarkably, in the FoxG1-Cre cKO, the DG
154 appears to be almost absent (Fig. 2A).

155 At the end of gestation, CRC, expressing Reelin (D'Arcangelo et al., 1995), and INP, expressing
156 Tbr2 (Hodge et al., 2013), have a characteristic organization in the hippocampus: CRC are localized
157 around the HF, while INP have migrated from the DNE, by the ventricle, along the DMS, have
158 reached the HF and are found below the CRC layer (see Fig. 1A). In the FoxG1-Cre cKO, Reelin
159 expression (marking CRC) is greatly reduced, and a HF is not observed (Fig. 2D); in Emx1-Cre
160 cKO, Reelin is reduced, but the HF is visible (Fig. 2E), and in Nestin-Cre cKO Reelin appears
161 slightly reduced, but with a normal-looking distribution around the HF (Fig. 2F). Similarly, Tbr2
162 expression is greatly reduced in FoxG1-Cre cKO; an initial dorsal migratory stream is visible, but
163 no DG is observed (Fig. 2G). Instead, in Emx1-Cre cKO, Tbr2-positive INP have reached the HF,
164 but their abundance is greatly reduced (Fig. 2H). On the other hand, in Nestin-Cre cKO, Tbr2-
165 positive INP appear to have completed their migration, and their abundance seems only slightly, if
166 at all, reduced (Fig. 2I).

167 To summarize, Sox2 ablation by E9.5 in the telencephalon in FoxG1-Cre cKO results, by the end of
168 gestation, in lack of DG formation, accompanied by a missing HF. Ablation just a day later, in
169 Emx1-Cre cKO, has much less dramatic effects: a hippocampal fissure forms, though CRC and INP
170 are reduced and the DG is much smaller compared to controls. Nestin-Cre cKO appear much less, if
171 at all, affected, as previously published (Favaro et al., 2009).

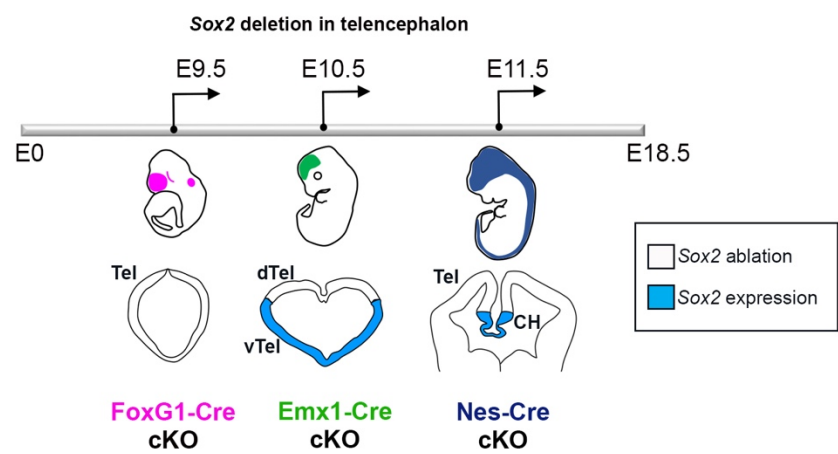
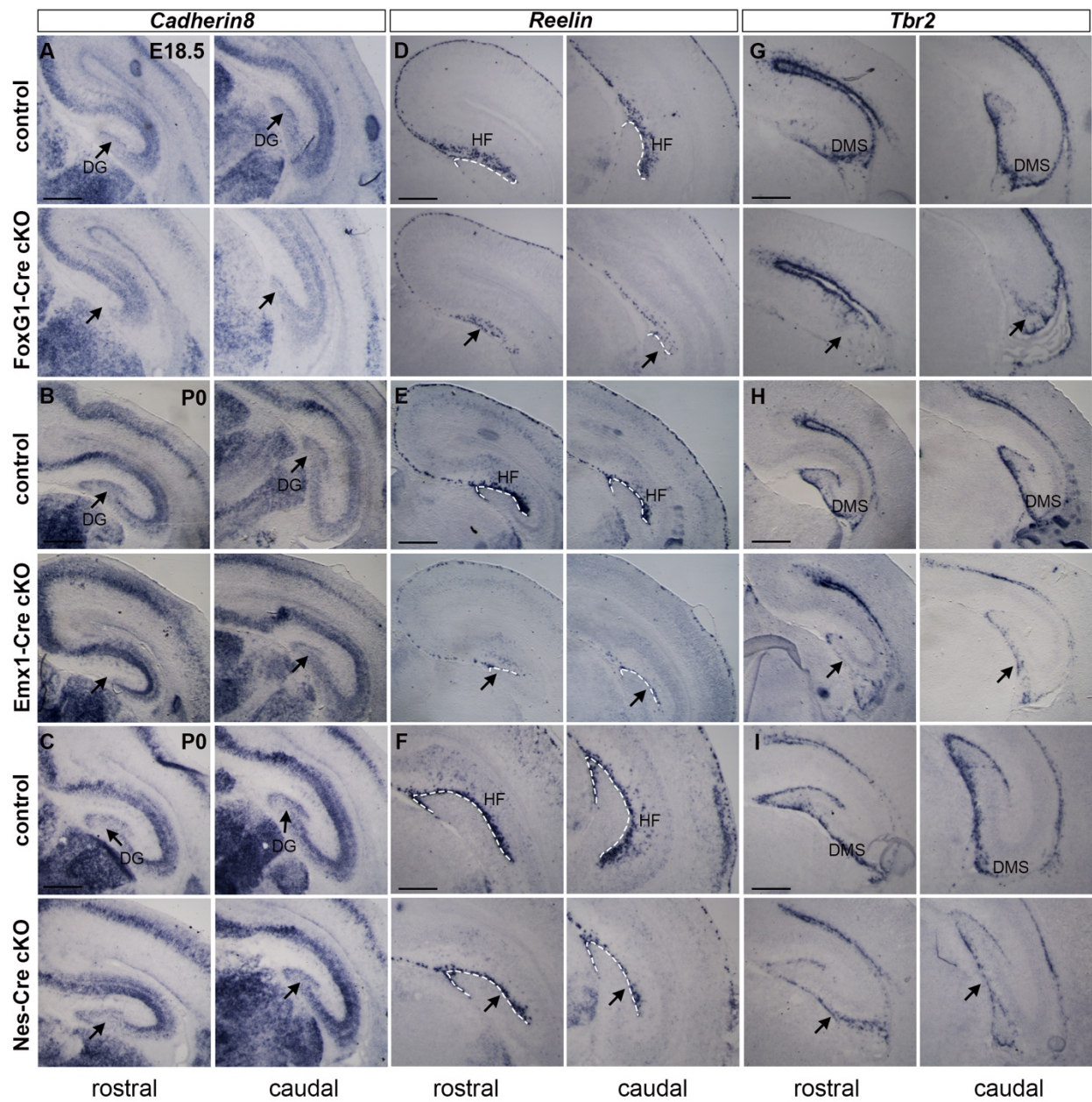


Figure 2

Hippocampus development is affected by Sox2 loss, the early Sox2 is ablated the stronger the phenotype observed.

In situ hybridization for *Cadherin8* (A-C), *Reelin* (D-F) and *Tbr2* (G-I) on coronal sections of control and Sox2 FoxG1-Cre cKO brains at E18.5 (A,D,G), control and Emx1-Cre cKO brains at P0 (B,E,H) and control and Nes-Cre cKO brains at P0 (C,F,I). At least 3 controls and 3 mutants were analyzed for each probe. A schematic representation of the timing of Sox2 ablation with the different Cre lines is at the bottom. Scale bars 200 μ m.

DG, dentate gyrus; HF, hippocampal fissure; DMS, dentate migratory stream; Tel, telencephalon; dTel, dorsal telencephalon; vTel, ventral telencephalon; CH, cortical hem.

Neural progenitors, differentiated neurons and radial glia are affected by Sox2 loss

We then characterized the development of specific hippocampal cell types in the most affected (FoxG1-Cre) mutants. Key for the morphogenesis of the hippocampus is the radial glia (RG) scaffold known to be required for the DMS to reach its final destination in the forming DG (Li, Kataoka, Coughlin, & Pleasure, 2009). By immunohistochemistry for GFAP, recognizing RG, at E18.5, we find that the RG scaffold in FoxG1-Cre cKO is completely disorganized (Fig. 3A). No morphologically identifiable DG is present, and the few RG found have random organization (Fig. 3A, arrows). At this same stage, different neuronal populations are normally found in the hippocampus: granule neurons in the DG, and pyramidal neurons forming the CA1, CA2 and CA3 regions. We performed ISH for NeuroD1, a marker of differentiated neurons; in FoxG1-Cre cKO, while NeuroD1-positive cells in the CA regions are present, NeuroD1-positive cells in the DG, abundant in controls, are almost absent in the mutant (Fig. 3B). In the DG, at this stage, neural stem/progenitor cells, marked by the expression of the Hes5 gene (Basak & Taylor, 2007), are normally present (see Fig. 3C, controls); in FoxG1-Cre cKO, however, very few Hes5-positive cells are found (Fig. 3C). In conclusion, early Sox2 loss in the telencephalon (FoxG1-Cre cKO) appears to lead to later reduction of both differentiated neurons and proliferating neural progenitors; in addition, the radial glia scaffold is completely disorganized.

The formation of the hippocampal fissure and the dentate migration require Sox2 expression from early developmental stages

After having identified the hippocampal defects present, in our mutants, at the end of gestation, we examined earlier developmental stages, to define the developmental history of the defects. We focused in particular on the FoxG1-Cre mutant, showing the most pronounced abnormalities (see Fig. 2).

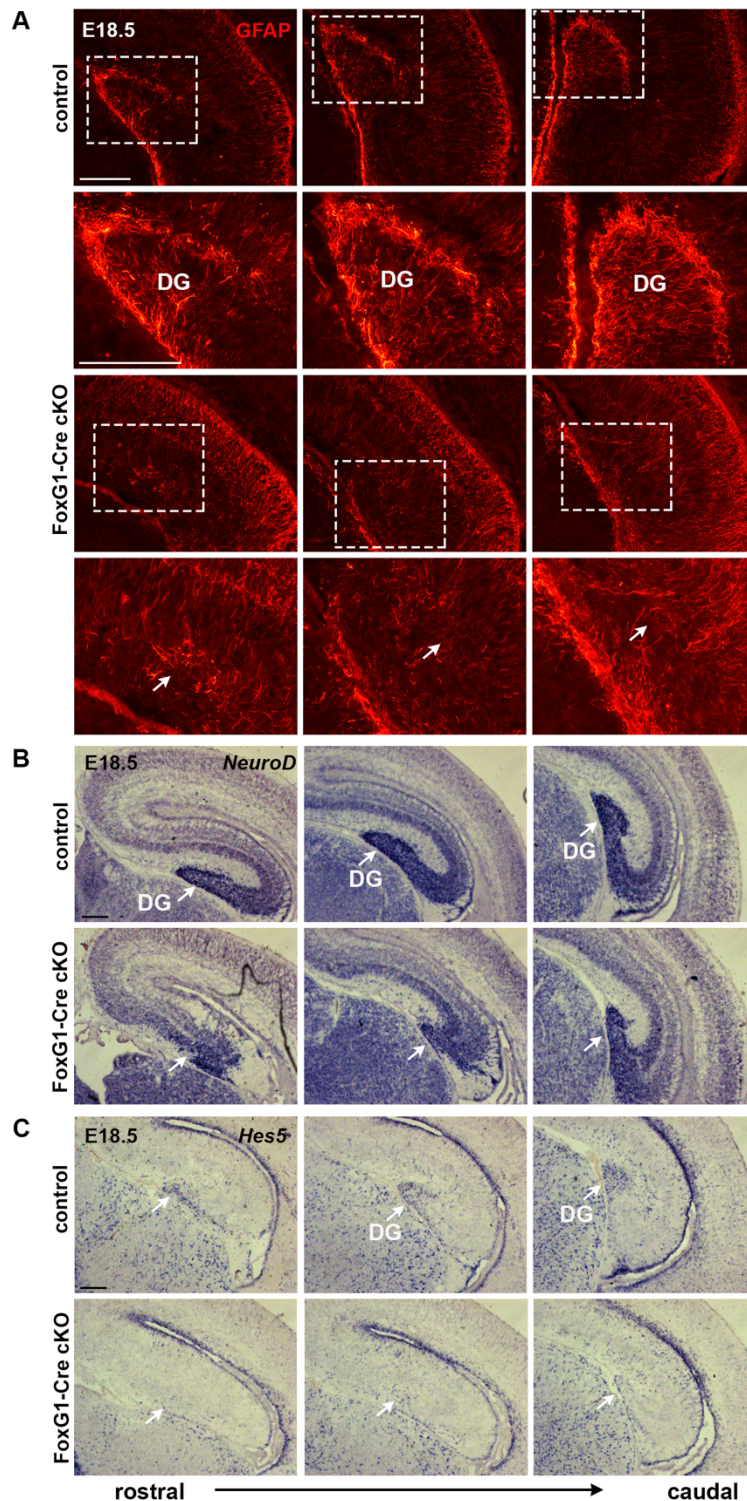


Figure 3

Radial glia formation, neuronal differentiation and neural stem cells formation is severely affected in FoxG1-Cre cKO.

(A) GFAP immunofluorescence at E18.5 on coronal sections of control and FoxG1-Cre cKO hippocampi (controls n=6, mutants n=4). (B,C) *In situ* hybridization at E18.5 for *NeuroD* (B) (controls n=4, mutants n=3) and *Hes5* (C) (controls n=2, mutants n=2) on coronal sections of control and FoxG1-Cre cKO hippocampi. Arrows indicate the underdeveloped dentate gyrus (DG) in cKO. Scale bars 200 μm.

219 A defect in distribution of CRC (marked by Reelin) and INP (marked by Tbr2) is apparent, at the
220 end of gestation, in Sox2 FoxG1-Cre and Emx1-Cre cKO (Fig. 2D,E,G,H). What happens in the
221 first steps of the development of the hippocampus to CRC and INP in these mutants? We addressed
222 this question by ISH with markers for these cell types at early developmental stages, in FoxG1-Cre
223 (Early) cKO embryos (Fig. 4). We also examined the expression of Cxcr4, a chemokine receptor
224 expressed in INP and neuroblasts in the DMS and in CRC, and its ligand Cxcl12, expressed by the
225 meninges, and required for the migration of INP and CRC (Berger, Li, Han, Paredes, & Pleasure,
226 2007; Borrell & Marin, 2006; Hodge et al., 2013; Li et al., 2009); we also examined P73, a P53
227 homolog, expressed by CRC and important for hippocampal fissure and DG formation (Meyer et
228 al., 2004; Meyer et al., 2019).

229
230 At E12.5, Tbr2 is expressed, in controls, by INP in the DNE and in CR cells towards the pia (Fig.
231 4A); in the FoxG1-Cre cKO mutant, whereas Tbr2 expression in CRC (towards the pia, arrow)
232 appears present, expression in the DNE is not detected (Fig. 4A). This might reflect a loss of Tbr2-
233 expressing INP; however, we do not observe changes in the number of proliferating cells in this
234 region at E12.5 by EdU labelling (Fig. S2), suggesting that at least some INP remain, but express
235 less Tbr2 or are mislocalized. P73, Reelin and Cxcr4 expression appears unaltered in mutants
236 compared to controls at this stage (Fig. 4B-D).

237
238 At E14.5, P73 and Reelin expression marks, in controls, CRC in the medial telencephalic wall
239 region where hippocampal morphogenesis will soon begin (Fig. 4E,F, arrow); in the mutant, a
240 strong reduction of P73 and Reelin expression is observed (Fig. 4E,F, arrow). Of note, this
241 reduction is detected specifically in the CH of FoxG1-Cre cKO (Fig. 4E,F), even though Sox2 is
242 ablated in the whole telencephalon. At this stage, also Cxcr4 expression in CRC appears reduced in
243 the CH of FoxG1-Cre cKO (Fig. 4G).

244
245 At E16.5, in controls, strong P73 and Reelin expression marks the hippocampal fissure (HF),
246 defining the beginning of overt hippocampal morphogenesis (Fig. 4H,I); in sharp contrast, this
247 expression is not seen or greatly reduced in the mutant (Fig. 4H,I). Cxcl12 is also expressed, in the
248 control, in the developing HF, and its expression is also lost in the mutant (Fig. 4K).
249 Concomitantly, Cxcr4 expression in the hippocampus primordium (HP) is also reduced (Fig. 4J).
250 These data point to a failure to initiate proper HF development in the mutant.

251 Interestingly, at E16.5, P73, Reelin and Cxcr4 expression is reduced throughout the telencephalon in
252 FoxG1-Cre cKO (Fig. 4).

253

254 At E18.5, P73 marks the HF in controls, but its expression is completely absent in the FoxG1-Cre
255 cKO brain, indicating a complete depletion of P73-positive CH-derived CRC (Fig. 4L). Cxcr4
256 expression in the DG and Cxcl12 expression in the HF is also greatly reduced in the mutant,
257 confirming a severe abnormality of the mutant hippocampus at the end of gestation (Fig. 4M,N).
258 In conclusion, the defects detected, at the end of gestation, in FoxG1-Cre mutants originate early in
259 development, with a failure, at early stages, to develop a HF and migrating DNE cells in these
260 mutants.

261

262 ***Genes essential for hippocampal development are downregulated following early (FoxG1-Cre***
263 ***cKO), but not late (Emx1-Cre cKO, Nestin-Cre cKO), Sox2 deletion***

264 Having observed that early Sox2 mutants (in particular FoxG1-Cre cKO) show severely defective
265 hippocampal development, we searched for Sox2-regulated downstream genes, whose deregulation
266 in mutants could explain the observed defects. We compared the expression of several candidate
267 genes in mutants and controls, at E12.5, a stage preceding the observed abnormalities (clearly
268 observed, in mutants, from E14.5, when hippocampal morphogenesis begins). Having observed that
269 the defects in early Sox2 mutants (FoxG1-Cre cKO) are much more severe than those arising in
270 later (Emx1-Cre and Nestin-Cre cKO) mutants, we reasoned that genes downstream to Sox2, that
271 are functionally relevant for these early defects, should show altered expression in early (FoxG1-
272 Cre) mutants, but not, or less, in later mutants (Emx1-Cre; Nestin-Cre).

273 We thus investigated the expression of genes, representing candidate mediators of Sox2 function, in
274 early and late mutants, by ISH.

275

276 Prime candidate genes to mediate defective hippocampal development in early Sox2 mutants
277 include genes encoding signalling molecules, expressed in the CH.

278 Key signaling molecules secreted by the CH and required for hippocampus formation are
279 components of the Wnt pathway; in fact, Wnt3a knock-out results in a complete loss of the
280 hippocampus (Lee, Tole, Grove, & McMahon, 2000). We analyzed what happens, at E12.5, to the
281 expression of Wnt3A in the three Sox2 cKO. We found that Wnt3A is severely downregulated
282 specifically in the CH of FoxG1-Cre cKO (Fig. 5A), but only slightly downregulated in Emx1-Cre
283 cKO (Fig. 5B), while it is only very mildly, if at all, reduced at this stage in the Nestin-Cre cKO

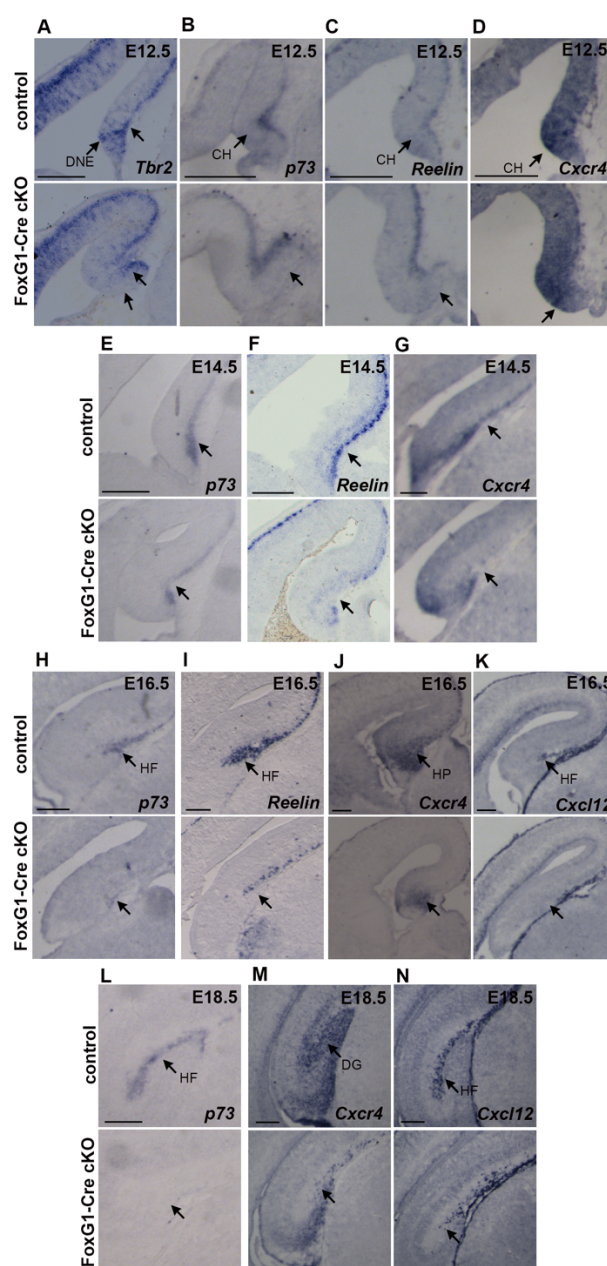


Figure 4
Expression of genes important for the development of the hippocampus is affected by Sox2 loss in FoxG1-Cre cKO.

(A-D) *In situ* hybridization at E12.5 on coronal sections of control and FoxG1-Cre cKO dorsal telencephalons for *Tbr2* (controls n=10, mutants n=10) (A), *P73* (controls n=3, mutants n=3) (B), *Reelin* (controls n=7, mutants n=6) (C) and *Cxcr4* (controls n=7, mutants n=7) (D). (E-G) *In situ* hybridization at E14.5 on coronal sections of control and FoxG1-Cre cKO brains for *P73* (controls n=3, mutants n=3) (E), *Reelin* (controls n=7, mutants n=5) (F) and *Cxcr4* (controls n=3, mutants n=3) (G). (H-K) *In situ* hybridization at E16.5 on coronal sections of control and FoxG1-Cre cKO hippocampi for *P73* (controls n=2, mutants n=2) (H), *Reelin* (controls n=6, mutants n=5) (I), *Cxcr4* (controls n=5, mutants n=4) (J) and *Cxcl12* (controls n=4, mutants n=3) (K). (L-N) *In situ* hybridization at E18.5 on coronal sections of control and FoxG1-Cre cKO hippocampi for *P73* (controls n=3, mutants n=3) (L), *Cxcr4* (controls n=5, mutants n=4) (M) and *Cxcl12* (controls n=5, mutants n=4) (N). Arrows indicate the downregulation of expression in the mutant cortical hem (CH), dentate neuroepithelium (DNE), hippocampal primordium (HP), dentate gyrus (DG) and hippocampal fissure (HF). Scale bars 200 μm.

(Fig. 5C). We analyzed the expression of another Wnt family member, Wnt2b in FoxG1-Cre cKO and Emx1-Cre cKO. While Wnt2b was strongly downregulated in the CH of FoxG1-Cre cKO (Fig. 5D), it was only slightly downregulated in the CH of Emx1-Cre cKO compared to controls (Fig. 5E). Wnt5A, another Wnt family member normally expressed in the CH, was instead expressed in the CH of FoxG1-Cre cKO (Fig. 5F), indicating that the CH, as a structure, is present in these mutants, though it fails to express Wnt3a and Wnt2b. Interestingly, expression of the transcription factor Lhx2, a marker of the cortex which is not expressed in the cortical hem, has a normal expression pattern in FoxG1-Cre cKO, including an Lhx2-non-expressing neuroepithelial region, suggesting that a CH is present in these mutants (Fig. 5G).

In conclusion, expression of components of the Wnt pathway known to be involved in the development of the hippocampus is strongly downregulated in the CH of FoxG1-Cre cKO, but not of Emx1-Cre cKO and Nestin-Cre cKO.

Other key genes for hippocampus formation include Gli3, encoding a transcription factor acting as a nuclear effector in the Shh signaling pathway. The knockout of Gli3 impairs the development of the hippocampus, where DG development is as severely affected as in our Sox2 early (FoxG1-Cre cKO) mutants. Of note, Gli3 acts, in hippocampal development, by regulating expression of components of the Wnt pathway (Grove, Tole, Limon, Yip, & Ragsdale, 1998). We found that Gli3 expression is specifically downregulated in the CH (though not in the cortex) of FoxG1-Cre cKO, but not of Emx1-Cre cKO and Nestin-Cre cKO (Fig. 5H-J).

Recent work from our laboratory identified SOX2 binding sites in an intron of the Gli3 gene in NSC cultured from the mouse forebrain; further, this intronic region is connected to the Gli3 promoter by a long-range interaction mediated by RNApolIII ((Bertolini et al., 2019) and Fig. 6A). A DNA segment, overlapping the SOX2 peak, drives expression of a lacZ transgene to the embryonic mouse forebrain ((Visel et al., 2009) and <https://enhancer.lbl.gov>) (Fig. 6A). We found that this Sox2-bound region, when connected to a minimal promoter and a luciferase reporter gene, and transfected in Neuro2a cells, is activated by increasing doses of a cotransfected Sox2-expressing vector in a dose-dependent way (Fig. 6B).

Cxcr4, downregulated in early (FoxG1Cre) Sox2 mutants at E14.5 (Fig. 4G), is also functionally involved in the development of the hippocampus (Discussion). Of note, an enhancer active in the developing brain, located within an intron of the Dars gene, but connected to the Cxcr4 gene

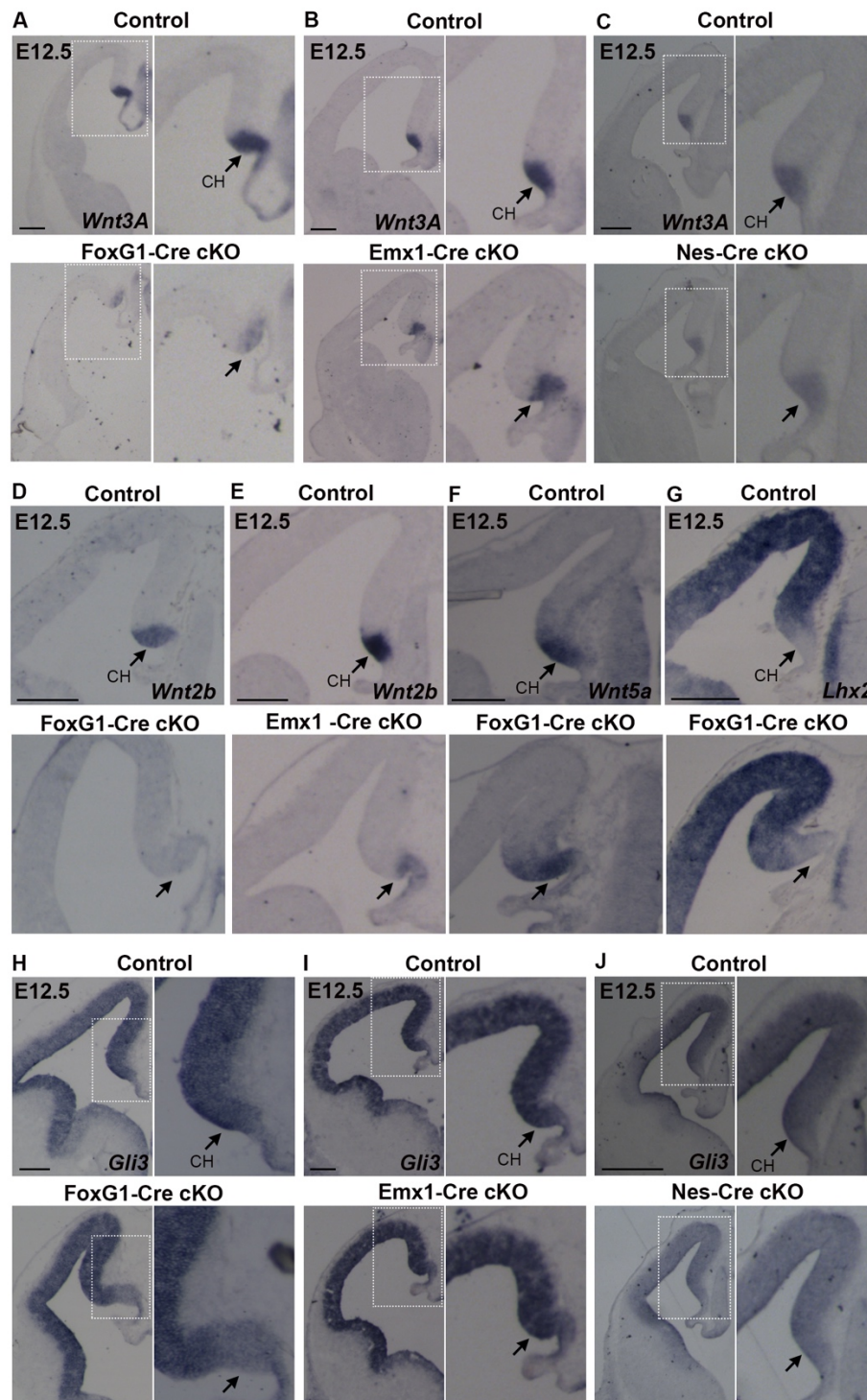


Figure 5

Expression of key molecules for hippocampal development is downregulated in the cortical hem of FoxG1-Cre cKO but mildly or not affected in Emx1- Cre or Nes-Cre cKO.

In situ hybridization at E12.5 for Wnt3A (A-C), Wnt2b (D,E), Wnt5A (F), Lhx2 (G), Gli3 (H-J) on control and FoxG1-Cre cKO (A,D,F,G,H), Emx1-Cre cKO (B,E,I) and Nes-Cre cKO (C,J) coronal brain sections. Arrows indicate the cortical hem (CH). At least 3 controls and 3 mutants were analyzed for each probe. Scale bars 200 μm.

342
343
344
345
346
347
348
349
350
351
352
353
354
355
356
357
358
359
360
361
362
363
364
365
366
367
368
369
370
371
372
373
374

promoter by a long-range interaction in brain-derived NSC chromatin, is bound by SOX2 in these cells (Bertolini et al., 2019) (Fig. 6C).

In conclusion, Sox2 early ablation leads to reduced expression, particularly in early (FoxG1-Cre) mutants, of several genes key to hippocampal development, some of which are directly bound and regulated by SOX2; some of these genes (Gli3, Wnt3a) are also known to functionally regulate each other (see Discussion). These genes may thus be considered as part of a Sox2-dependent gene regulatory network, controlling hippocampal development (Fig. 6D; see Discussion).

Emx1-Cre mediated Sox2 ablation alters the excitatory input in CA3 and CA1 pyramidal neurons

We also wished to ask about the consequences of Sox2 early loss on the physiological functioning of the postnatal hippocampus.

As illustrated earlier (Fig. 2A, 2B), early Sox2 loss causes DG hypoplasia, most severe in FoxG1-cKO mutants, but clearly present also in Emx1-Cre cKO mice. Since FoxG1-cKO are perinatally lethal (A. Ferri et al., 2013), we performed physiology studies on Emx1-cKO mutants. We addressed, in particular, the function of CA3 and CA1 pyramidal neurons, central to hippocampal circuitry and relatively spared, morphologically at least, in our mutants (in comparison to the severely hypoplastic DG).

The DG receives its main extrinsic input from the entorhinal cortex and is the first hippocampal station of the classical trisynaptic pathway: entorhinal cortex → DG granule cells → CA3 pyramidal neurons → CA1 pyramidal neurons. The DG projects exclusively to CA3 through mossy fibers. In turn, CA3 projects to CA1 through Schaffer collaterals (Witter & Amaral, 2004). Hence, we investigated whether the hypoplastic DG in our Emx1-Cre mutants could alter signal transfer to CA3 and CA1. This hypothesis was tested by studying intrinsic excitability and excitatory transmission in CA3/CA1 pyramidal neurons. These were first identified by their typically large pyramidally-shaped soma (~20 μm diameter, in CA3), and then further distinguished by their action potential firing. We focused on regular-spiking pyramidal neurons, the widest population, characterized by slow firing with modest adaptation and excitability properties consistent with literature on CA1-CA3 neurons in mice (e.g., (Hunt, Linaro, Si, Romani, & Spruston, 2018; Venkatesan, Liu, & Goldfarb, 2014)). A typical example is shown in Fig. 7A. The excitability features of pyramidal neurons from control and mutant mice are shown in Supplementary Table 1,

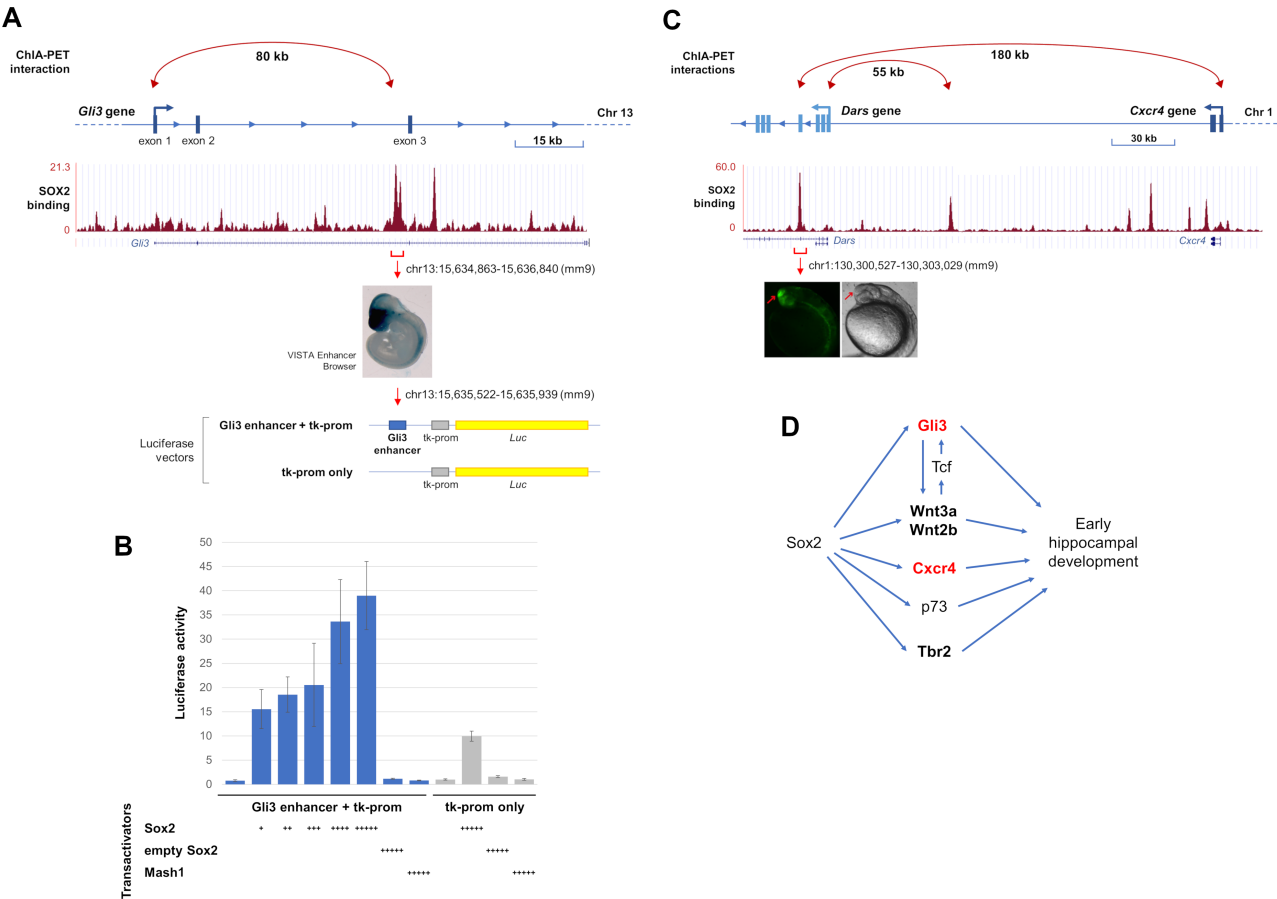


Figure 6

SOX2 acts on distal enhancers and on long-range enhancer-promoter interactions of several genes key to hippocampal development, and activates a Gli3 intronic enhancer in a dose-dependent way

(A) Diagram of the Gli3 gene, and SOX2-binding profile across the Gli3 locus in NSC (ChIPseq data from (Bertolini et al., 2019)). A Sox2-dependent 80kb long-range interaction connects the Gli3 promoter with a SOX2-bound region, in the second intron (ChIA-PET data from (Bertolini et al., 2019)). This region acts as a brain-specific enhancer in E10.5 mouse embryo (image from <https://enhancer.lbl.gov/>); it was cloned into the depicted luciferase vector, upstream to a minimal tk promoter, to address its responsivity to Sox2.

(B) Enhancer activation assay in Neuro2a cells transfected with the constructs in (A): Gli3 enhancer + tk-promoter (blue histograms), or tk-promoter only (grey histograms). Cotransfection of these constructs with increasing amounts of a Sox2-expressing vector (Sox2, X axis), but not of a control “empty” vector (empty Sox2), or a Mash1-expressing vector (Mash1), resulted in dose-dependent increase of luciferase activity (Y axis) driven by the Gli3 enhancer + tk-prom vector, but not the tk-prom only vector. The molar ratios, compared with the luciferase vector (set at 1) were: +, 1:0.050; ++, 1:0.075; +++, 1:0.125; +++, 1:0.25; +++, 1:0.5. Results are represented as fold-change increase in activity compared with the tk-prom only vector, which is set at 1. Values are the mean of two (for Sox2+ and Sox2++) or three (other samples) independent experiments carried out in triplicate. Error bars represent standard deviation.

(C) Diagram of the Cxcr4 gene, reporting SOX2 binding and Sox2-dependent long-range interactions in NSC (as in A for Gli3; data from (Bertolini et al., 2019)). Note that the Cxcr4 promoter is connected to a SOX2-bound region within the intron of a different gene, Dars; this region acts as a brain-specific enhancer in transgenic zebrafish embryos (picture from (Bertolini et al., 2019)).

(D) A model depicting the activation, by Sox2, of different genes key to hippocampal development (present paper), some of which cross-regulate each other; in red, direct SOX2 targets; in bold, early expressed hippocampal regulators, downregulated already at early stages in Sox2 mutants (see Discussion).

while the stimulus/frequency relations are shown in [Fig. 7B](#). Overall, little difference was observed in intrinsic excitability between mutant and control mice, in both CA1 and CA3.

In these neurons, we recorded the spontaneous excitatory post-synaptic currents (EPSCs) for 10 min after reaching the whole-cell configuration, at -68 mV. Spontaneous EPSCs reflect the overall excitatory input impinging on a given pyramidal neuron. Typical EPSC traces from CA3 pyramidal neurons are shown in [Fig. 7C](#), for controls and mutants. Somewhat surprisingly, EPSC frequencies in CA3 displayed a ~30% increase in mutant animals compared to the controls ([Fig. 7E](#)). On the contrary, the average EPSC median amplitudes were not different between control and mutant mice ([Fig. 7E](#)). Moreover, the EPSC amplitudes obtained from all control and mutant cells were pooled in [Fig. 7F](#). The amplitude distributions of the two genotypes were compared with KS test, which revealed no significant difference.

Next, we studied the excitatory input onto CA1, which is the last station of the hippocampal serial pathway of information transfer. Typical EPSC traces are shown in [Fig. 7D](#) for control and mutant. As expected (Traub, Jefferys, & Whittington, 1999), the overall EPSC frequency and amplitude tended to be smaller in CA1, compared to CA3. The average EPSC frequencies in CA1 are reported for control and mutant mice in [Fig. 7G](#). Data reveal an approximately 50% reduction in mutant animals compared to the controls. Once again, little difference between genotypes was observed in the EPSC amplitudes ([Fig. 7G, H](#)).

In conclusion, CA3/CA1 pyramidal neuron firing or EPSC amplitudes were not altered in *Emx1-Cre cKO* mice, arguing against a direct effect of the mutation on the synaptic machinery or intrinsic excitability, which is consistent with the lack of expression of *Sox2* in these neurons (data not shown). However, EPSC frequency increased in CA3 and was approximately halved in CA1 of mutant mice, suggesting that excitatory signal transfer along the canonical trisynaptic pathway was unbalanced as a consequence of the major impairment of DG development produced by early *Sox2* ablation.

Overall, our data indicate significant functional alterations of the hippocampal circuitry in early *Sox2* mutants, which might plausibly contribute to the epileptic and cognitive defects in human patients (see Discussion).

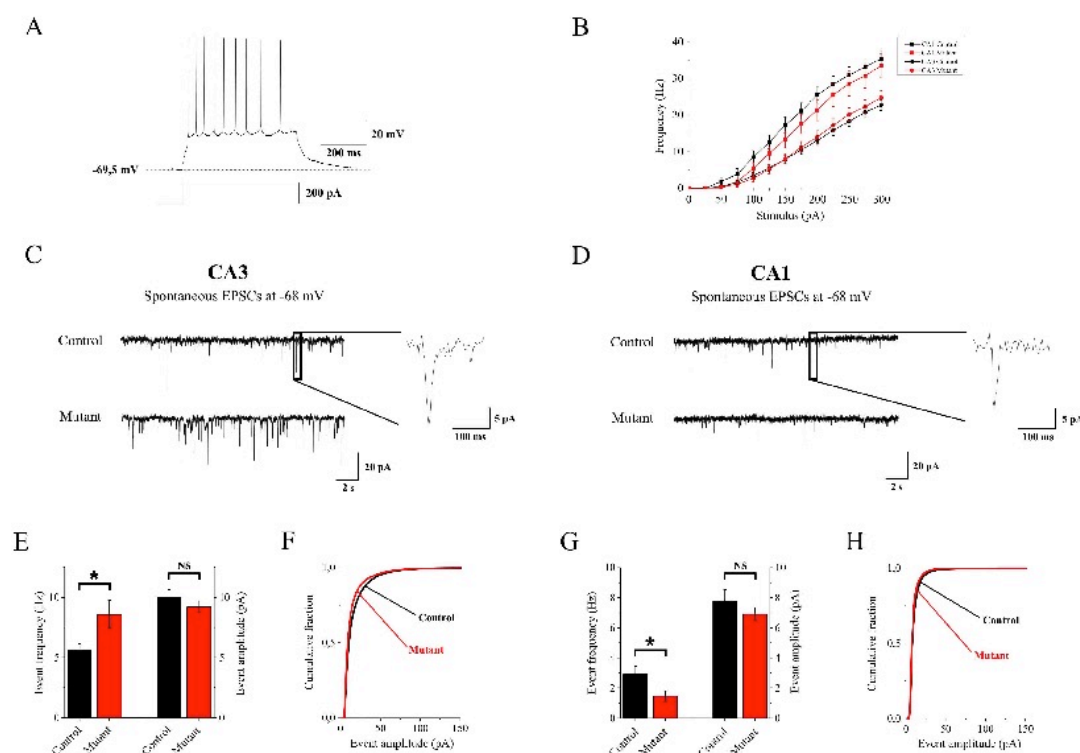


Figure 7

In Emx1-Cre cKO mice, excitatory transmission is altered in CA3 and CA1 hippocampal regions.

Early Sox2 ablation leads to alterations in the excitatory input onto both CA3 and CA1 pyramidal neurons. (A) Typical firing response to a 200 pA stimulus of injected current in a CA3 pyramidal neuron. (B) Average stimulus/frequency relation for hippocampal pyramidal neurons recorded in CA3 (Circles) and CA1 (Squares). No major differences were observed between control (Black) and mutant animals (Red). (C and D) EPSCs traces, at -68 mV, recorded in simulated physiologic conditions onto pyramidal neurons in CA3 and CA1 region respectively. *Insets*. Magnification of a representative EPSC event. (E) Average EPSCs frequencies and median amplitudes observed in CA3 pyramidal neurons recorded from 15 animals between p19 and p31. In mutant animals, Sox2 ablation induced a significant increase in EPSCs frequency compared to controls (8.60 ± 1.15 Hz, $n = 20$ and 5.59 ± 0.57 Hz, $n = 28$ respectively; $p = 0.03941$, with Mann-Whitney test), whereas, no significant effect was produced on event amplitudes (9.21 ± 0.47 pA, $n = 20$ and 10.01 ± 0.61 pA, $n = 28$ respectively). (F) Amplitude distribution of the total amount of collected EPSCs showing no major differences between control and mutant mice. (G) In CA1, EPSCs frequency significantly decreased in mutant animals compared to controls (1.46 ± 0.35 Hz, $n = 13$ and 2.91 ± 0.52 Hz, $n = 13$ respectively; $p = 0.02745$, with Mann-Whitney test). No difference in the average median amplitude was observed (controls: 7.75 ± 0.69 pA, $n = 20$ and mutants: 6.92 ± 0.44 pA, $n = 28$). (H) The amplitude distribution of the total pool of events recorded from 13 animals between p19 and p31 showed no major alterations between control and mutant mice.

Discussion

In this work, we highlighted an early time window in hippocampal development, where the Sox2 transcription factor is necessary to initiate the embryogenesis of the hippocampus. In fact, following Sox2 mutation with FoxG1-Cre, active from E8.5 (A. Ferri et al., 2013; Hébert & McConnell,

2000), hippocampal development is drastically defective, with a nearly complete absence of the DG; DG development is also defective, but present, following mutation with Emx1-Cre, active from E10.5; Sox2 mutation with Nestin-Cre has very little effect on hippocampal embryogenesis (Fig. 2).

These observations point to gene regulatory events, orchestrated by Sox2, that are required to initiate hippocampal development; at least some of these events are likely to be direct effects of SOX2 (Fig. 6). What is the nature of these events?

Gene regulatory events mediating early Sox2 function in hippocampal development

A severe reduction in the early expression of key regulators of hippocampal development (Wnt3a; Gli3; Cxcr4; Tbr2; p73) is observed in early Sox2 mutants (FoxG1-Cre cKO), already at early stages of hippocampal embryogenesis (E12.5, E14.5), preceding the overt phenotypic manifestation of the defect (hippocampal morphogenesis begins at about E14.5) (Figs. 4,5). Of note, reduced expression in the mutant CH at E12.5 is seen for some genes (e.g. Wnt3a, Gli3) but not others (Wnt5a; Fig. 5), suggesting that the CH is present, but dysfunctional in directing hippocampal formation. Importantly, a reduction in expression of these master genes is also observed in Emx1-Cre mutants, but to a lesser extent than in FoxG1-Cre mutants (Fig. 5). These observations suggest that the differential reduction in the expression of these key regulators accounts, at least in part, for the differences in the severity of the hippocampal embryogenesis defects between the three mutants.

What molecular mechanisms cause the differential expression of master hippocampal regulator genes between different mutants?

SOX2 is able to directly bind to at least some of these target genes (Gli3, Cxcr4, Fig. 6A,C) in neural cells chromatin, and to act as a transcriptional activator on some SOX2-bound enhancers (Gli3) within these loci (Fig. 6B), suggesting that it is directly involved in the transcriptional activation of at least some of these genes during hippocampal development. Further, SOX2-bound distant enhancers within the Gli3 and Cxcr4 loci are connected to the gene promoter in a Sox2-dependent way, at least in NSC (Fig. 6A,C), indicating that SOX2 may contribute to their regulation also through this “architectural” function (Bertolini et al., 2019; Wei, Nicolis, Zhu, & Pagin, 2019).

At E12.5 and afterwards, Sox2 is ablated in both FoxG1-Cre and Emx1-Cre mutants, yet critical genes are much more downregulated in FoxG1-Cre mutants, in agreement with a requirement for Sox2 to properly initiate the expression of these genes at early stages. We speculate that SOX2 may

act at early stages to initiate the organization of a 3D interaction network connecting gene promoters to enhancers (Fig. 6A,C), as a prerequisite for gene expression, in agreement with previous findings in NSC (Bertolini et al., 2019; Wei et al., 2019).

Altered regulation of a gene regulatory network of hippocampal master genes leads to defective cell development and cell-cell signaling in early Sox2 mutants, and eventually to defective hippocampal structure and function

The failure to properly activate early-acting hippocampal master genes may provide a molecular explanation to the failure to develop, in early Sox2 mutants, cell types essential in hippocampal development, or to prevent their proper behavior, as observed in Figs. 2,3.

In FoxG1-Cre, but not in Emx1-Cre Sox2 mutants, the Gli3 gene is downregulated at early stages (E12.5) in the segment of medial telencephalic wall required for hippocampal development, the CH (Fig. 5H,I). Gli3 encodes a transcription factor, and its homozygous mutation (as in the *extra-toes* Gli3^{Xt/Xt} mouse mutant) leads to absence of the hippocampus (Li & Pleasure, 2014; Theil, Alvarez-Bolado, Walter, & Ruther, 1999). In Gli3 mutant embryos, the medial wall of the telencephalon fails to invaginate to initiate hippocampal development, pointing to an early defect of the proliferating neuroepithelial cells of the prospective hippocampus (Li & Pleasure, 2014; Theil et al., 1999). Mutations of human GLI3 cause Pallister-Hall syndrome and Greig cephalopolysyndactyly syndrome, a complex defect that can involve seizures and intellectual disability, though hippocampal abnormalities were not specifically investigated (Naruse, Ueta, Sumino, Ogawa, & Ishikiriya, 2010). In mouse Gli3 mutants, the expression of Wnt signaling molecules, normally expressed in the CH, including Wnt3a and Wnt2b, is lost, and Wnt signaling is impaired at early stages of hippocampal development (Fotaki, Price, & Mason, 2011; Grove et al., 1998; Theil, Aydin, Koch, Grotewold, & Ruther, 2002).

The expression of Wnt3a and Wnt2b, encoding secreted signaling molecules produced by the CH signaling center, is also defective in early Sox2 mutants (Fig. 5); their downregulation is most pronounced in FoxG1-Cre mutants, less so in Emx1-Cre mutants (see above and Fig. 5A,B,D,E). The downregulation of Gli3 may contribute to this (see above).

Wnt signaling exerts its effects on target cells by inducing nuclear translocation of beta-catenin, that acts as a transcriptional regulator associating with TCF transcription factors; mutation of TCF

factors, e.g. Lef1, leads to failure of hippocampal development (Galceran, Miyashita-Lin, Devaney, Rubenstein, & Grosschedl, 2000; Li & Pleasure, 2014; Roelink, 2000). Of note, TCF binding regulates (Hasenpusch-Theil et al., 2012) the same intronic Gli3 enhancer, that we found to be bound and activated by Sox2 (Fig. 6A,B), suggesting that this element may integrate the effects of Wnt signaling and SOX2 activity in controlling Gli3 expression. Interestingly, Sox2/TCF binding sites were also described to act on other genes in the context of a transcriptional switch accompanying chromatin remodeling during neuronal differentiation (Muotri et al., 2010).

We attempted to reactivate the Wnt pathway in the FoxG1-Cre cKO, by LiCl injection, to see if we could rescue any of the observed defects. We found some amelioration of the organization and number of CRC in the cortex (Fig. S3B,C), although the overall hippocampus development remained defective (Fig. S3A,C). We also tried to reactivate the Wnt pathway by a Wnt agonist (AZD 1080); a partial rescue of Reelin retention in the CH, usually observed in mutants, was observed at E14.5 in the FoxG1-Cre cKO (Fig. S3D). We hypothesized that earlier treatment might have had more pronounced effects, however this resulted in high embryonic lethality, preventing us to observe the effects.

In conclusion, we propose that loss of Wnt signaling from the CH represents one mechanism whereby Sox2 early loss causes defective hippocampal embryogenesis likely by regulating the production of CRC. Assessing the relative contribution of this mechanism will be postponed to future studies.

We detected, in our early mutants, reduced expression of Tbr2, Cxcr4, Cxcl12 and p73, marking specific cell types in hippocampal embryogenesis (Fig. 4). However, knock-out experiments previously demonstrated that these genes, further to marking specific cell types (see Fig. 2), also play functional roles in hippocampal (as well as neocortical) development (Bagri et al., 2002; Hodge et al., 2013; Lu, Grove, & Miller, 2002; Meyer et al., 2004; Mimura-Yamamoto et al., 2017). This suggests that their reduced expression in Sox2 mutants may also functionally contribute to the hippocampal defects.

Cxcr4, whose expression is downregulated at early stages in Sox2 early mutants (Fig. 4G), is essential in particular for the development of the DG (Lu et al., 2002; Mimura-Yamamoto et al., 2017). Cxcr4 encodes a cell surface receptor, expressed in Granule Cell Progenitors (GCP) of the developing hippocampus, that also express GFAP (Mimura-Yamamoto et al., 2017). In hippocampal development, GCP, arising in the ventricular zone (DNE), migrate (dentate migratory

stream) to the subpial region, to form the granule cell layer (GCL) of the DG (Fig. 1A). The production and migration of GCP is regulated by various signaling molecules, including CXCL12 (the CXCR4 ligand), Reelin, Wnt, and BMP proteins, secreted by regions surrounding the developing DG. In the absence of Cxcr4, the numbers of dividing cells in the migratory stream and the prospective DG is dramatically reduced (Lu et al., 2002). It thus seems plausible that Cxcr4 deficiency importantly contributes to the impaired development of GFAP-positive GCP, and the consequent failure to develop a DG, seen in our early Sox2 mutants. P73 encodes a transcription factor expressed in differentiating CRC (Fig. 4), the choroid plexus and the ependyma (Meyer, Schaaps, Moreau, & Goffinet, 2000; Yang et al., 2000) and its knock-out in mice results in a phenotype very similar to the early loss of Sox2 in FoxG1-Cre cKO, with a lack of HF and almost absent DG (Meyer et al., 2019). P73 has a similar expression pattern in the fetal human brain suggesting a role in hippocampus development also in humans (Meyer et al., 2019). Interestingly, Reelin-expressing CRC in Sox2 mutants are similarly reduced in number and they may be retained in the cortical hem instead of moving towards the pia. P73 has a very restricted expression pattern, but its knock-out has a broad effect on cortical patterning suggesting it could be involved in the signaling activities of the CH (Meyer et al., 2004).

Radial scaffold, Cajal-retzius cells and lack of hippocampal fissure and dentate gyrus

One of the key outcomes of early ablation of Sox2 in the developing telencephalon, via FoxG1-Cre, is the lack of the hippocampal fissure followed by an extreme reduction of the DG. Radial glia scaffold disorganization due to knock-out of the transcription factor Nflb leads to lack of a specific hippocampal GFAP-positive glial population, lack of hippocampal fissure and DG without affecting cell proliferation, CRC differentiation or Wnt signalling (Barry et al., 2008); this suggests that the loss and disorganization of GFAP-positive cells, seen in our mutants specifically in the developing hippocampus (Fig. 3), might constitute a cellular mechanism contributing to the defective DG development in early Sox2 mutants.

Knock-out of P73 in CH-derived CRC cells leads to lack of hippocampal fissure and DG, as previously mentioned (Meyer et al., 2004). CRC are known to regulate RG formation both in the cortex and in the developing hippocampus (Forster et al., 2002; Frotscher, Haas, & Forster, 2003); conversely, RG has been shown to be important for the correct positioning of CRC cells (Kwon, Ma, & Huang, 2011). Our data suggests that Sox2 does not regulate proliferation in the medial telencephalon at E12.5 (Fig. S2); it is possible that it regulates aspects of differentiation of RG and CRC.

Functional alteration of hippocampal circuitry in Sox2-ablated mice

In Emx1-Cre Sox2-deleted mice, we observed functional alterations in the excitatory transmission along the serial transmission pathway of the hippocampal formation, and particularly an imbalance in the excitatory input onto CA3 and CA1 pyramidal neurons (Fig. 7). Considering that i) the main effects of Sox2 ablation are produced during hippocampal embryogenesis, ii) Sox2 is not expressed in CA3/CA1 neurons, iii) Sox2 deletion caused negligible alterations in pyramidal neuron excitability and excitatory synaptic efficacy, we attribute most of the observed functional effects to altered maturation of the connectivity pattern of hippocampal formation. Neural circuits in the hippocampal formation comprise both serial and parallel pathways. DG is regulated by cortical input from entorhinal layer III, and projects to CA3. However, entorhinal layer III also projects to CA3. Moreover, CA3 displays profuse recurrent reciprocal connections between pyramidal neurons (Witter & Amaral, 2004). Therefore, the higher EPSC frequency we observed in CA3 pyramidal neurons of Sox2-deleted mice could be caused by: i) a denser innervation from entorhinal layer III, permitted by the lower entorhinal input to the hypoplastic DG; ii) an increased recurrent collateral connectivity between CA3 cells, fostered by the absence of the physiological stimulus from DG; iii) a decreased recurrent inhibition on CA3 pyramidal cells, as mossy fibers from DG also regulate GABAergic interneurons in CA3 (Acsady, Kamondi, Sik, Freund, & Buzsaki, 1998). We cannot presently distinguish between these mechanisms, which are not mutually exclusive. Nonetheless, the increased excitatory input we observed in CA3 pyramidal cells is consistent with the epileptic phenotype frequently associated with the brain malformations caused by Sox2 mutations (Sisodiya et al., 2006). Considering the peculiar propensity of CA3 region to develop seizure-like activity (de la Prida, Huberfeld, Cohen, & Miles, 2006; Miles & Wong, 1983), we hypothesize that increased excitatory activity in CA3 of Sox2-deleted mice could facilitate seizure onset, perhaps through CA3 projection to septal areas (Colom, 2006; Swanson & Cowan, 1977). By contrast, the excitatory input on CA1 pyramidal neurons was lower in Emx1-Cre cKO mice. This could be caused by increased local feed-back inhibition by GABAergic neurons, because of overstimulation by the overactive CA3 fibers. Alternatively, in the absence of proper DG input, the partial disorganization of CA3 connectivity could favor recurrent collaterals at the expense of Schaffer collaterals. Regardless of the specific mechanism, our results demonstrate that Sox2 ablation at early developmental stages unbalances the normal CA3 to CA1 excitatory input, which could contribute to explain some of the cognitive alterations observed in Sox2 mutants. Although early Sox2 ablation leads to severe DG hypoplasia, many cognitive functions can be carried out

even when hippocampal volume is strongly reduced (Moser & Moser, 1998; Sisodiya et al., 2006). It is therefore not surprising that the effects of Sox2 ablation on cognition of viable animals are subtle. Nonetheless, evidence is available in humans about a variety of cognitive alterations associated with Sox2 mutations (Ragge et al., 2005; Sisodiya et al., 2006). In general, CA1 is the main output channel of the hippocampal formation, and is thought to compare the entorhinal cortex input (conveying the present state of the environment) with the CA3 input (conveying mnemonic representations of expected events based on external signals; (Knierim & Neunuebel, 2016). Our results suggest that Sox2 malfunction may cause cognitive damage by altering such comparative function of CA1.

Conclusion and perspective

Overall, our work shows that Sox2 controls (directly, or indirectly) the activity of multiple, functionally interconnected genes, forming a gene regulatory program active and required at very early stages of hippocampal development. Reduced activity of this program leads to essentially absent (FoxG1-Cre mutants) or reduced (Emx1-Cre mutants) development of the hippocampus, in particular the DG. In the Emx1 mutants, which are viable, hippocampal physiology is importantly perturbed. These findings may provide novel perspectives for therapy approaches of genetic brain disease rooted in defective hippocampal development.

Materials and methods

Mouse strains

Mutant mice were obtained by crossing the Sox2Flox (Favaro et al., 2009) line with the following lines: FoxG1-Cre (Hébert & McConnell, 2000), Emx1-Cre (Gorski et al., 2002) and Nestin-Cre; Sox2 β Geo (Tronche et al., 1999);Medina, 2004 #506;Favaro, 2009 #3}. The mouse line Sox2-CreERT2 (Favaro et al., 2009), was crossed to a transgenic mouse line with a *loxP-EYFP* reporter of Cre activity (Rosa26R-EYFP) (Srinivas et al., 2001) to determine the progeny of Sox2 expressing cells following tamoxifen injection (as described below). The day of vaginal plug was defined as embryonic day 0 (E0) and the day of birth as postnatal day 0 (P0). Genotyping of adult mice or embryos was performed with the following primers: Sox2 Flox Forward: 5' AAGGTACTGGGAAGGGACATTT 3'

659 Sox2 Flox Reverse: 5'AGGCTGAGTCGGGTCAATTA 3'
 660 FoxG1-Cre Forward: 5' AGTATTGTTTTGCCAAGTTCTAAT 3'
 661 FoxG1-Cre Reverse: 5'AGTATTGTTTTGCCAAGTTCTAAT 3'
 662 Emx1-Cre IRES Forward: 5'AGGAATGCAAGGTCTGTTGAAT 3'
 663 Emx1-Cre IRES Reverse: 5' TTTTCAAAGGAAAACACGTC 3'
 664 Nestin-Cre Forward: 5' CGCTTCCGCTGGGTCACCTGTCG 3'
 665 Nestin-Cre Reverse: 5' TCGTTGCATCGACCGGTAATGCAGGC 3'
 666 R26R-EYFP Forward: 5' TTCCCGCACTAACCTAATGG 3'
 667 R26R-EYFP Reverse: 5' GAACTTCAGGGTCAGCTTGC 3'
 668 Sox2-CreERT2 Forward: 5' TGATCCTACCAGACCCTTCAGT 3'
 669 Sox2-CreERT2 Reverse: 5' TCTACACATTTTCCCTGGTTCC 3'

670 The FoxG1-Cre mouse line was maintained in 129 background as recommended in (Hébert &
 671 McConnell, 2000). The other mouse lines were maintained in a mixed background enriched in
 672 C57BL/6 and DBA.

673 All procedures were in accordance with the European Communities Council Directive (2010/63/EU
 674 and 86/609/EEC), the National Institutes of Health guidelines, and the Italian Law for Care and Use
 675 of Experimental Animals (DL26/14). They were approved by the Italian Ministry of Health and the
 676 Bioethical Committees of the University of Milan-Bicocca.

677

678

679 *In situ hybridization*

680 *In situ* hybridization was performed essentially as in (Mercurio et al., 2019). Briefly, embryonic
 681 brains and P0 brains were dissected and fixed overnight (O/N) in paraformaldehyde 4% in PBS
 682 (Phosphate Buffered Saline; PFA 4%) at 4°C. The fixed tissue was cryoprotected in a series of
 683 sucrose solutions in PBS (15%, 30%) and then embedded in OCT (Killik, Bio-Optica) and stored at
 684 -80°C. Brains were sectioned (20 µm) with a cryostat, placed on a slide (Super Frost Plus 09-
 685 OPLUS, Menzel) and stored at -80°C. Slides were then defrosted, fixed in formaldehyde 4% in
 686 PBS for 10 minutes (min), washed 3 times for 5 min in PBS, incubated for 10 min in acetylation
 687 solution (for 200 ml: 2.66 ml triethanolamine, 0.32 ml HCl 37%, 0.5 ml acetic anhydride 98%) with
 688 constant stirring and then washed 3 times for 5 min in PBS. Slides were placed in a humid chamber
 689 and covered with prehybridization solution (50% formamide, 5X SSC, 0.25 mg/ml tRNA, 5X
 690 Denhardt's, 0.5 µg/ml salmon sperm) for at least 2 hours (h) and then incubated in hybridization
 691 solution (fresh prehybridization solution containing the digoxigenin (DIG)-labelled RNA probe of

interest) O/N at 65°C. Slides were washed 5 min in 5X SSC, incubated 2 times in 0.2X SSC for 30 min at 65°C, washed 5 min in 0.2X SSC at room temperature (RT) and then 5 min in Maleic Acid Buffer (MAB, 100 mM maleic acid, 150 mM NaCl pH 7.5). The slides were incubated in blocking solution (10% sheep serum, 2% blocking reagent (Roche), 0.3% Tween-20 in MAB) for at least 1 h at RT, then covered with fresh blocking solution containing anti-DIG antibody Roche © 1:2000 and finally placed O/N at 4°C. Slides were washed in MAB 3 times for 5 min, in NTMT solution (100 mM NaCl, 100 mM Tris-HCl pH 9.5, 50 mM MgCl₂, 0.1% Tween-20) 2 times for 10 min and then placed in a humid chamber, covered with BM Purple (Roche), incubated at 37°C until desired staining was obtained (1-6 h), washed in water for 5 min, air dried and mounted with Eukitt (Sigma).

The following DIG-labelled probes were used: *Sox2* (Avilion et al., 2003), *Cadherin8* (Korematsu & Redies, 1997), *Tbr2* (Bulfone et al., 1999), *Reelin* (a gift from Luca Muzio, HSR Milan), *Cxcr4* (Lu et al., 2002), *Cxcl12* (Lu et al., 2002), *Wnt3A* (Grove et al., 1998), *Wnt2b* (Grove et al., 1998), *Wnt5a* (Grove et al., 1998), *Gli3* (a gift from Luca Muzio, HSR Milan), *Lhx2* (a gift from Shubha Tole, Tata Institute Mumbai), *P73* (a gift from Olivia Hanley, UZH). The *P73* probe was transcribed directly from a PCR product, obtained from E12.5 cDNA, with the following primers: Forward 5' AGCAGCAGCTCCTACAGAGG 5' and Reverse 5' TAATACGACTCACTATAGGGCCTTGGGAAGTGAAGCACTC 3' (which includes the T7 promoter underlined).

Immunohistochemistry

Immunohistochemistry was performed essentially as in (Cerrato et al., 2018). Brains were dissected, fixed, embedded and sectioned as for *in situ* hybridization, except for fixation in PFA4% that was often 3-4h at 4°C. Sections were washed in PBS 5 min, unmasked in citrate buffer (Na Citrate 0.01M, Citric acid 0.01M pH6) by boiling in a microwave 3 min and then washed in PBS 10 min at RT. Sections were blocked with blocking solution (FBS 10%, Triton 0.3%, PBS1X) for 1h at RT, then incubated O/N in blocking solution with primary antibodies: anti-mSOX2 (R&D Systems MA2018, 1:50), anti-P73 (Neomarkers, 1:150), anti-Reelin (Millipore MAB5364, 1:500), anti-Tuj1 (Covance, 1:400), anti-GFP (Invitrogen A10262, 1:500, used to detect EYFP expressing cells), anti-GFAP (Dako, 1:500). Slides were then washed in PBS 2 times, 10 min each, and incubated in blocking solution containing the secondary fluorescent antibody (1:1000, Alexa Fluor Invitrogen) for 1h 30 minutes at RT. Slides were then washed in PBS twice, 10 minutes each, and then mounted with Fluormount (F4680, Sigma) with 4',6-diamidino-2-phenylindole (DAPI) and imaged with a

725 confocal microscope (Nikon A1R) and with a Zeiss Axioplan 2 Fluorescent microscope for anti-
726 GFAP immunostainings.

727

728 *Lineage tracing of progeny of Sox2 expressing progenitors*

729 R26R-EYFP females were crossed with Sox2-CreERT2 males. E9.5 pregnant females were injected
730 intraperitoneally with tamoxifen (20 mg ml⁻¹ in ethanol/corn oil 1:10, 0.1 mg per g of body weight)
731 that induces Cre recombinase activity in the Sox2 telencephalic expression domain (Favaro et al.,
732 2009) and therefore turns on EYFP in this expression domain. Embryos were collected at E15.5,
733 fixed in 4% PFA O/N, embedded in OCT and sectioned at the cryostat (20-µm sections) as for *in*
734 *situ* hybridization (see above).

735 *EdU tracing*

736 Ethynyldeoxyuridine (EdU, Molecular Probes) was injected in E12.5 pregnant females at 50 µg/g
737 body weight. Embryos were collected 30 min after injection, fixed O/N in PFA 4% and embedded
738 for cryostat sectioning as above. Edu incorporation was detected on sections (20 µm) with the
739 Click-iT EdU Kit Alexa Fluor 594 (C10354, Thermo Fisher) following manufacturer's instructions.
740 Briefly, slides were washed twice in PBS 2 min each and incubated for 20 min at RT in Triton 0.5%
741 in PBS. Slides were then washed in Triton 0.1% in PBS 3 times, 3 min each. Sections were
742 incubated 30 min in the dark with EdU Click reaction according to manufacturer's instructions.
743 Slides were then washed in PBS 3 times 5 min, stained with DAPI, mounted with Fluoromount
744 (F4680, Sigma) and imaged with a confocal microscope (Nikon A1R). The number of EdU positive
745 cells in the cortical hem and dentate neuroepithelium was counted on at least 3 consecutive coronal
746 sections for each brain. Data are represented as mean ± standard deviation.

747

748 *Brain slices*

749 For patch-clamp experiments, coronal sections (300 µm thick) containing the hippocampal region (-
750 1.22 mm to -2.70 mm from bregma) were prepared from mice of both sexes (6M and 10F) aged P19-
751 P31, by applying standard procedures (Aracri, Meneghini, Coatti, Amadeo, & Becchetti, 2017).

752

753 *Patch-clamp recording and data analysis*

Cells were examined with an Eclipse E600FN direct microscope, equipped with water immersion DIC objective (Nikon Instruments, Milano, Italy), and digital CCD C8484-05G01 IR camera with HCLImage Live acquisition software (Hamamatsu Photonics Italia, Arese, Italy). Stimulation and recording were carried out in whole-cell mode, by using a Multiclamp 700A amplifier (Molecular Devices, Sunnyvale, CA), at 33-34°C. Borosilicate capillaries (OD 1.5 mm; Corning Inc., NY) were pulled (2-3 MΩ) with a Flaming/Brown P-97 micropipette puller (Sutter Instruments, Novato, CA). Series resistance after patch rupture was usually around 10-15 MΩ and was compensated up to at least 70%. Cell capacitance was also compensated. Synaptic currents and action potentials were low-pass filtered at 2 kHz and digitized at 5 kHz with Digidata 1322A / pClamp 9.2 (Molecular Devices). During recording, slices were perfused (~2 ml/min) with artificial cerebrospinal fluid, containing (mM): 135 NaCl, 21 NaHCO₃, 0.6 CaCl₂, 3 KCl, 1.25 NaH₂PO₄, 1.8 MgSO₄, 10 D-glucose, aerated with 95% O₂ and 5% CO₂ (pH 7.4). Pipette contained (mM): 140 K-gluconate, 5 KCl, 1 MgCl₂, 0.5 BAPTA, 1 MgATP, 0.3 NaGTP, 10 HEPES (pH 7.26). Resting membrane potential (V_{rest}) was determined in open circuit mode ($I=0$), immediately after reaching the whole-cell configuration. No correction was applied for liquid junction potentials. Series resistance was monitored throughout the experiment by applying small stimuli around V_{rest} . Cells were discarded when R_s was higher than 15 MΩ.

Action potentials and EPSCs were analysed with Clampfit 9.2 (Molecular Devices), MiniAnalysis, and OriginPro 9.1 (OriginLab Corporation, Northampton, MA, USA), as previously reported (Aracri, Amadeo, Pasini, Fascio, & Becchetti, 2013; Aracri et al., 2017).

AZD and LiCl treatment

AZD 1080 (Axon Medchem, Axon Catalog ID: 2171) diluted in ascorbic acid 0.5%/EDTA 0.01%, was administered to pregnant females once a day by oral gavage from E9.5 to E12.5. We administered 5 µl AZD/g of body weight (AZD 0.375 µg/µl at E9.5 and E10.5, AZD 0.75 µg/µl at E11.5 and E12.5). Embryos were then collected at E14.5. Ascorbic acid 0.5%/EDTA 0.01% was administered as a control.

LiCl, or NaCl as a control, were injected intraperitoneally in pregnant female from E9.5 to E14.5 or from E10.5 to E12.5 once a day at the same time. No difference was observed between the two injection time windows. 10 µl/g of body weight of 600 mM LiCl or 600 mM NaCl were injected. Embryos were collected at E18.5 and processed for *in situ* hybridization. Injection of AZD 1080 or LiCl in pregnant females at E8.5 led to abortions.

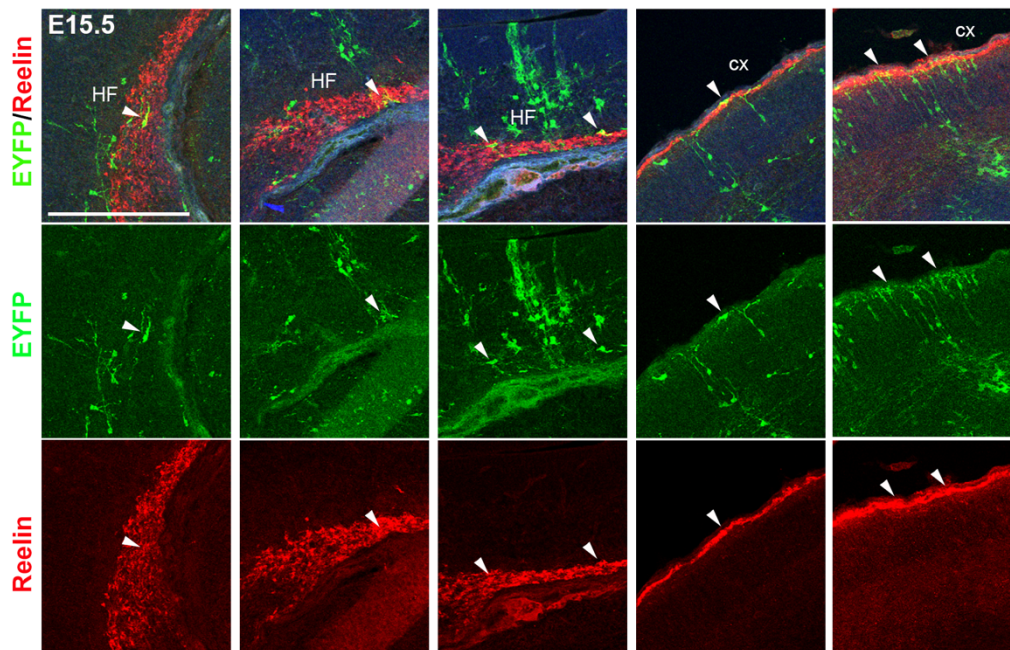
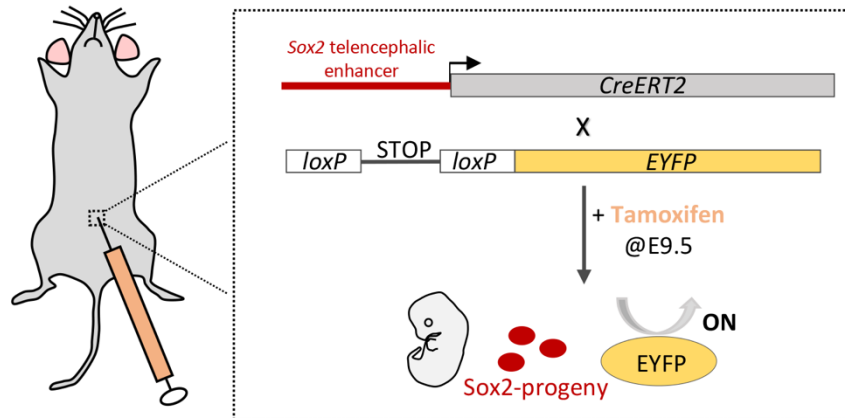
The number of *Reelin*-positive cells at the hippocampal fissure and in the cortex was counted using Photoshop CC 2015 on five consecutive coronal sections of each brain. Data are represented as mean \pm standard deviation and were statistically analyzed using unpaired Student's T-test, *** $p < 0.005$.

Luciferase constructs

The DNA region in the Gli3 second intron overlapping the SOX2 peak, and corresponding to the VISTA enhancer (coordinates under the embryo in Fig. 6A) was PCR-amplified from the vector where it had been cloned upstream to the lacZ reporter (a gift from T. Theil; (Hasenpusch-Theil et al., 2012)), and cloned upstream to the tk promoter in the Tk-luc vector (Mariani et al., 2012), into the KpnI and NheI restriction sites.

Transfection experiments

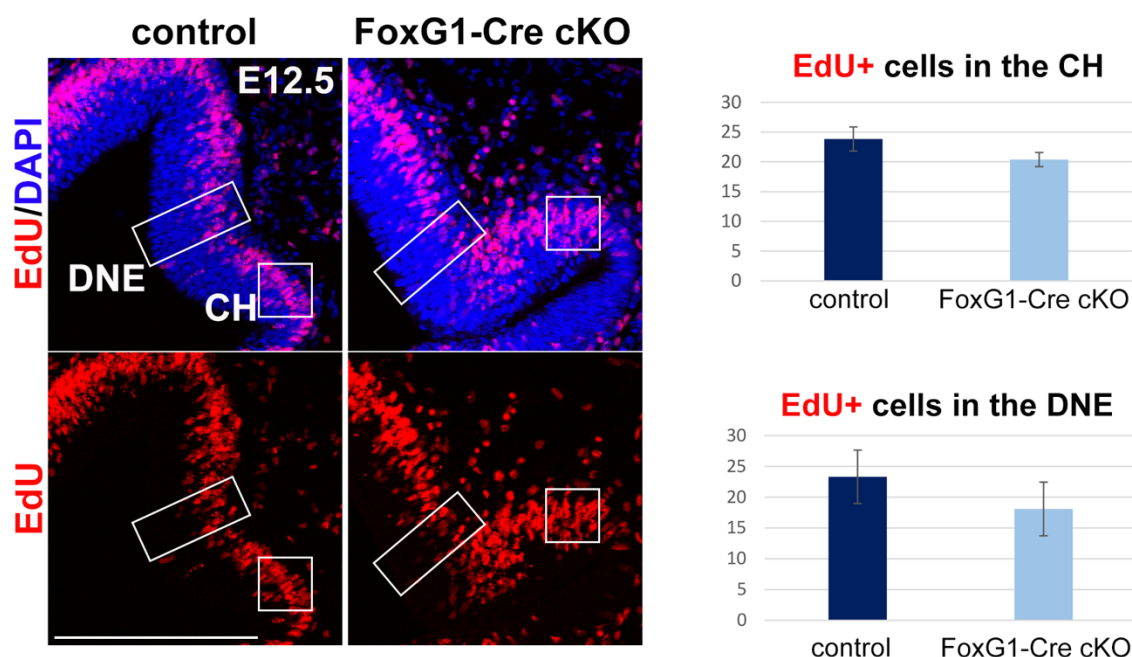
The transfection experiments were performed essentially as previously described (Mercurio et al., 2019; Panaliappan et al., 2018). In particular, Neuro-2a cells were plated in Minimal Essential Medium Eagle (MEM; SIGMA), supplemented with 10% Foetal Bovine Serum, L-Glutamine, penicillin and streptomycin. For transfection, cells were plated in 12-well plates at 1.5×10^5 cells/well, and transfected on the following day using Lipofectamine 2000 (Invitrogen). Briefly, medium in each well was replaced with 1 ml of MEM medium (with no addition) mixed with 2 μ l of Lipofectamine 2000, and DNA. After 4 hours from transfection, the medium was replaced with complete medium. A fixed amount of 300 ng of luciferase reporter plasmid was used for each well, with increasing amounts of Sox2 expressing vector (Favaro et al., 2009; Mariani et al., 2012), or the corresponding control "empty" vector (not containing the transcription factor's cDNA), in the following luciferase vector:expressing vector molar ratios (indicated in Fig.6): +, 1:0.050; ++, 1:0.075; +++, 1:0.125; +++, 1:0.25; +++, 1:0.5. The pBluescript vector was added to transfection DNA to equalize the total amount of transfected DNA to a total of 800 ng for each reaction. After 24 hours, total cellular extracts were prepared, and Luciferase activity was measured with a Promega Luciferase Assay System, according to the manufacturer's instructions.



Supplementary Figure 1 **Lineage tracing of Sox2 expressing progeny in CR cells in the hippocampal fissure (HF) and the cortex.**

Top, scheme depicting the mouse crosses used to trace the progeny of Sox2 expressing cells. A mouse in which expression of an inducible Cre recombinase (cre-ERT2) was under the control of a Sox2 telencephalic enhancer was crossed to a mouse in which YFP expression would be turned on when Cre recombinase was expressed, following tamoxifen injection.

Bottom, immunofluorescence for GFP (green) and Reelin (red) on coronal sections of brains at E15.5 from pregnant females injected with tamoxifen at E9.5. Arrows indicate cells that are positive for both GFP and Reelin in the hippocampal fissure (HF) and the cortex (cx). Scale bar 200 μm.



830

831

832

833

834

835

836

837

838

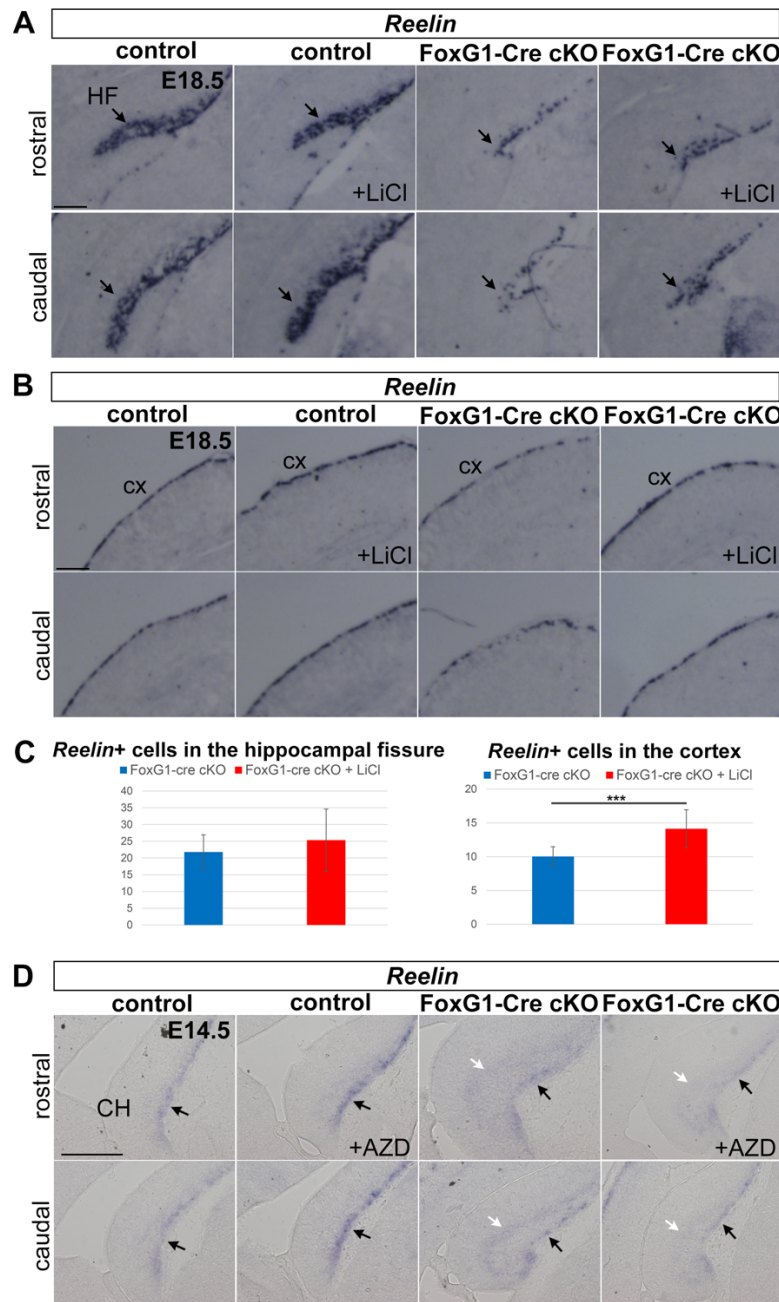
839

840

Supplementary Figure 2

Sox2 early ablation does not appear to affect cellular proliferation neither in the cortical hem nor in the dentate neuroepithelium

EdU staining on coronal sections of control and FoxG1-Cre cKO mice at E12.5 injected with EdU and sacrificed 30 minutes later. The graphs on the right show no significant difference in the number of proliferating cells in the cortical hem (CH) and in the dentate neuroepithelium (DNE) at the developmental stage analysed. Data are represented as mean \pm standard deviation (controls n=3, mutants n=3). Scale bar 200 μ m.



841

842

843

844

845

846

847

848

849

850

851

852

853

854

Supplementary Figure 3

Administration of agonists of the Wnt pathway LiCl and AZD 1080 partially rescues the deficit of C-R cells in the cortex, but only slightly in the hippocampal fissure.

Reelin in situ hybridization on coronal sections of control or FoxG1-Cre cKO brains injected with Wnt agonists, at the times indicated, and analyzed at E18.5 in the case of LiCl injection (A,B) and at E14.5 for AZD 1080 injection (D). LiCl or NaCl were intraperitoneally injected once a day in pregnant females from E10.5 to E12.5. AZD 1080 was administered by oral gavage once a day in pregnant females from E9.5 to E12.5. At least 3 controls and 3 mutants, both treated and untreated, were analyzed. The graphs in (C) indicate a significant rescue in the number of C-R cells in the cortex following LiCl injection (***) $p < 0.005$, unpaired Student's T-test. Mutants untreated $n = 5$, mutants LiCl treated $n = 5$. Error bars represent standard deviation. (D) Black arrows indicate *Reelin* expressing cells towards the pial side of the cortical hem, white arrows indicate *Reelin* expressing cells retained in the cortical hem that did not move towards the pia. AZD 1080 treatment rescued this retention. Scale bars 200 μ m.

Excitability features of CA1/CA3 pyramidal neurons of Emx1-Cre cKO and control mice.

Genotype	V _{rest} (mV)	Rheobase (pA)	1 st spike width (ms)	2 nd spike width (ms)	AHP (mV)	1 st to 2 nd spike interval (ms)	4 th to 5 th spike interval (ms)
CA1							
WT	-69.0 ±0.47	92.7 ±6.6	1.22 ±0.04	1.29 ±0.04	-4.16 ±0.6	25.2 ±3.0	42.8 ±3.8
Emx1-Cre cKO	-69.1 ±0.23	100.0 ±5.7	1.26 ±0.05	1.32 ±0.05	-5.11 ±1.2	34.2 ±3.9	59.4 ±6.0
CA3							
WT	-69.7 ±0.23	100.0 ±5.9	1.09 ±0.02	1.17 ±0.02	-5.7 ±0.4	39.4 ±4.3	73.9 ±6.7
Emx1-Cre KO	-69.8 ±0.18	110.0 ±6.4	1.16 ±0.04	1.24 ±0.04	-5.4 ±0.5	36.2 ±1.9	73.7 ±5.8

Supplementary Table 1

Excitability features of CA1/CA3 pyramidal neurons of Emx1-Cre cKO and control mice.

For the WT and Emx1-Cre cKO mice, the main excitability features are given for CA3 and CA1 pyramidal neurons, as indicated. The table reports average V_{rest}, rheobase, spike widths (measured at half-amplitude) of the first and second action potential, and AHP amplitude (with respect to V_{rest}). As a measure of firing adaptation, the time intervals are reported between the first and second spike and the fourth and fifth spike.

References

- Acsady, L., Kamondi, A., Sik, A., Freund, T., & Buzsaki, G. (1998). GABAergic cells are the major postsynaptic targets of mossy fibers in the rat hippocampus. *The Journal of neuroscience : the official journal of the Society for Neuroscience*, 18(9), 3386-3403. Retrieved from <https://www.ncbi.nlm.nih.gov/pubmed/9547246>
- Aracri, P., Amadeo, A., Pasini, M. E., Fascio, U., & Becchetti, A. (2013). Regulation of glutamate release by heteromeric nicotinic receptors in layer V of the secondary motor region (Fr2) in the dorsomedial shoulder of prefrontal cortex in mouse. *Synapse*, 67(6), 338-357. doi:10.1002/syn.21655
- Aracri, P., Meneghini, S., Coatti, A., Amadeo, A., & Becchetti, A. (2017). alpha4beta2(*) nicotinic receptors stimulate GABA release onto fast-spiking cells in layer V of mouse prefrontal (Fr2) cortex. *Neuroscience*, 340, 48-61. doi:10.1016/j.neuroscience.2016.10.045
- Avilion, A. A., Nicolis, S. K., Pevny, L. H., Perez, L., Vivian, N., & Lovell-Badge, R. (2003). Multipotent cell lineages in early mouse development depend on SOX2 function. *Genes & development*, 17(1), 126-140. doi:10.1101/gad.224503
- Bagri, A., Gurney, T., He, X., Zou, Y. R., Littman, D. R., Tessier-Lavigne, M., & Pleasure, S. J. (2002). The chemokine SDF1 regulates migration of dentate granule cells. *Development*, 129(18), 4249-4260. Retrieved from <https://www.ncbi.nlm.nih.gov/pubmed/12183377>
- Barry, G., Piper, M., Lindwall, C., Moldrich, R., Mason, S., Little, E., . . . Richards, L. J. (2008). Specific glial populations regulate hippocampal morphogenesis. *The Journal of neuroscience : the official journal of the Society for Neuroscience*, 28(47), 12328-12340. doi:10.1523/JNEUROSCI.4000-08.2008
- Basak, O., & Taylor, V. (2007). Identification of self-replicating multipotent progenitors in the embryonic nervous system by high Notch activity and Hes5 expression. *The European journal of neuroscience*, 25(4), 1006-1022. doi:10.1111/j.1460-9568.2007.05370.x
- Berg, D. A., Su, Y., Jimenez-Cyrus, D., Patel, A., Huang, N., Morizet, D., . . . Bond, A. M. (2019). A Common Embryonic Origin of Stem Cells Drives Developmental and Adult Neurogenesis. *Cell*, 177(3), 654-668 e615. doi:10.1016/j.cell.2019.02.010
- Berger, O., Li, G., Han, S. M., Paredes, M., & Pleasure, S. J. (2007). Expression of SDF-1 and CXCR4 during reorganization of the postnatal dentate gyrus. *Developmental neuroscience*, 29(1-2), 48-58. doi:10.1159/000096210
- Bertolini, J. A., Favaro, R., Zhu, Y., Pagin, M., Ngan, C. Y., Wong, C. H., . . . Wei, C. L. (2019). Mapping the Global Chromatin Connectivity Network for Sox2 Function in Neural Stem Cell Maintenance. *Cell stem cell*, 24(3), 462-476 e466. doi:10.1016/j.stem.2019.02.004
- Borrell, V., & Marin, O. (2006). Meninges control tangential migration of hem-derived Cajal-Retzius cells via CXCL12/CXCR4 signaling. *Nature neuroscience*, 9(10), 1284-1293. doi:10.1038/nn1764
- Bulfone, A., Martinez, S., Marigo, V., Campanella, M., Basile, A., Quaderi, N., . . . Ballabio, A. (1999). Expression pattern of the Tbr2 (Eomesodermin) gene during mouse and chick brain development. *Mechanisms of development*, 84(1-2), 133-138. doi:10.1016/s0925-4773(99)00053-2

911 Cerrato, V., Mercurio, S., Leto, K., Fuca, E., Hoxha, E., Bottes, S., . . . Nicolis, S. K. (2018). Sox2
912 conditional mutation in mouse causes ataxic symptoms, cerebellar vermis hypoplasia, and
913 postnatal defects of Bergmann glia. *Glia*, 66(9), 1929-1946. doi:10.1002/glia.23448
914 Colom, L. V. (2006). Septal networks: relevance to theta rhythm, epilepsy and Alzheimer's disease.
915 *J Neurochem*, 96(3), 609-623. doi:10.1111/j.1471-4159.2005.03630.x
916 D'Arcangelo, G., Miao, G. G., Chen, S. C., Soares, H. D., Morgan, J. I., & Curran, T. (1995). A protein
917 related to extracellular matrix proteins deleted in the mouse mutant reeler. *Nature*,
918 374(6524), 719-723. doi:10.1038/374719a0
919 de la Prida, L. M., Huberfeld, G., Cohen, I., & Miles, R. (2006). Threshold behavior in the initiation
920 of hippocampal population bursts. *Neuron*, 49(1), 131-142.
921 doi:10.1016/j.neuron.2005.10.034
922 Fantes, J., Ragge, N. K., Lynch, S. A., McGill, N. I., Collin, J. R., Howard-Peebles, P. N., . . . FitzPatrick,
923 D. R. (2003). Mutations in SOX2 cause anophthalmia. *Nature genetics*, 33(4), 461-463.
924 doi:10.1038/ng1120
925 Favaro, R., Valotta, M., Ferri, A. L., Latorre, E., Mariani, J., Giachino, C., . . . Nicolis, S. K. (2009).
926 Hippocampal development and neural stem cell maintenance require Sox2-dependent
927 regulation of Shh. *Nature neuroscience*, 12(10), 1248-1256. doi:10.1038/nn.2397
928 Ferri, A., Favaro, R., Beccari, L., Bertolini, J., Mercurio, S., Nieto-Lopez, F., . . . Nicolis, S. K. (2013).
929 Sox2 is required for embryonic development of the ventral telencephalon through the
930 activation of the ventral determinants Nkx2.1 and Shh. *Development*, 140(6), 1250-1261.
931 doi:10.1242/dev.073411
932 Ferri, A. L., Cavallaro, M., Braidà, D., Di Cristofano, A., Canta, A., Vezzani, A., . . . Nicolis, S. K.
933 (2004). Sox2 deficiency causes neurodegeneration and impaired neurogenesis in the adult
934 mouse brain. *Development*, 131(15), 3805-3819. doi:10.1242/dev.01204
935 Forster, E., Tielsch, A., Saum, B., Weiss, K. H., Johanssen, C., Graus-Porta, D., . . . Frotscher, M.
936 (2002). Reelin, Disabled 1, and beta 1 integrins are required for the formation of the radial
937 glial scaffold in the hippocampus. *Proceedings of the National Academy of Sciences of the*
938 *United States of America*, 99(20), 13178-13183. doi:10.1073/pnas.202035899
939 Fotaki, V., Price, D. J., & Mason, J. O. (2011). Wnt/beta-catenin signaling is disrupted in the extra-
940 toes (Gli3(Xt/Xt)) mutant from early stages of forebrain development, concomitant with
941 anterior neural plate patterning defects. *The Journal of comparative neurology*, 519(9),
942 1640-1657. doi:10.1002/cne.22592
943 Frotscher, M., Haas, C. A., & Forster, E. (2003). Reelin controls granule cell migration in the
944 dentate gyrus by acting on the radial glial scaffold. *Cerebral cortex*, 13(6), 634-640.
945 doi:10.1093/cercor/13.6.634
946 Galceran, J., Miyashita-Lin, E. M., Devaney, E., Rubenstein, J. L., & Grosschedl, R. (2000).
947 Hippocampus development and generation of dentate gyrus granule cells is regulated by
948 LEF1. *Development*, 127(3), 469-482. Retrieved from
949 <https://www.ncbi.nlm.nih.gov/pubmed/10631168>
950 Gorski, J. A., Talley, T., Qiu, M., Puellas, L., Rubenstein, J. L., & Jones, K. R. (2002). Cortical
951 excitatory neurons and glia, but not GABAergic neurons, are produced in the Emx1-
952 expressing lineage. *The Journal of neuroscience : the official journal of the Society for*
953 *Neuroscience*, 22(15), 6309-6314. doi:20026564
954 Grove, E. A. (2008). Neuroscience. Organizing the source of memory. *Science*, 319(5861), 288-289.
955 doi:10.1126/science.1153743

- Grove, E. A., Tole, S., Limon, J., Yip, L., & Ragsdale, C. W. (1998). The hem of the embryonic cerebral cortex is defined by the expression of multiple Wnt genes and is compromised in Gli3-deficient mice. *Development*, 125(12), 2315-2325. Retrieved from <http://www.ncbi.nlm.nih.gov/pubmed/9584130>
- Hasenpusch-Theil, K., Magnani, D., Amaniti, E. M., Han, L., Armstrong, D., & Theil, T. (2012). Transcriptional analysis of Gli3 mutants identifies Wnt target genes in the developing hippocampus. *Cerebral cortex*, 22(12), 2878-2893. doi:10.1093/cercor/bhr365
- Hébert, J. M., & McConnell, S. K. (2000). Targeting of cre to the Foxg1 (BF-1) locus mediates loxP recombination in the telencephalon and other developing head structures. *Developmental biology*, 222(2), 296-306. doi:S0012-1606(00)99732-X [pii] 10.1006/dbio.2000.9732
- Hodge, R. D., Garcia, A. J., 3rd, Elsen, G. E., Nelson, B. R., Mussar, K. E., Reiner, S. L., . . . Hevner, R. F. (2013). Tbr2 expression in Cajal-Retzius cells and intermediate neuronal progenitors is required for morphogenesis of the dentate gyrus. *The Journal of neuroscience : the official journal of the Society for Neuroscience*, 33(9), 4165-4180. doi:10.1523/JNEUROSCI.4185-12.2013
- Hunt, D. L., Linaro, D., Si, B., Romani, S., & Spruston, N. (2018). A novel pyramidal cell type promotes sharp-wave synchronization in the hippocampus. *Nature neuroscience*, 21(7), 985-995. doi:10.1038/s41593-018-0172-7
- Kandel, E. R., Schwartz, J. H., & Jessell, T. M. (2000). *Principles of neural science* (4th ed.). New York: McGraw-Hill, Health Professions Division.
- Knierim, J. J., & Neunuebel, J. P. (2016). Tracking the flow of hippocampal computation: Pattern separation, pattern completion, and attractor dynamics. *Neurobiology of Learning and Memory*, 129, 38-49. doi:10.1016/j.nlm.2015.10.008
- Kondoh H, L.-B. R. e. b. (2016). *Sox2, Biology and Role in Development and Disease* (Vol. ISBN: 978-0-12-800352-7): Elsevier, Associated Press.
- Korematsu, K., & Redies, C. (1997). Expression of cadherin-8 mRNA in the developing mouse central nervous system. *The Journal of comparative neurology*, 387(2), 291-306. Retrieved from <https://www.ncbi.nlm.nih.gov/pubmed/9336230>
- Kwon, H. J., Ma, S., & Huang, Z. (2011). Radial glia regulate Cajal-Retzius cell positioning in the early embryonic cerebral cortex. *Developmental biology*, 351(1), 25-34. doi:10.1016/j.ydbio.2010.12.026
- Lee, S. M., Tole, S., Grove, E., & McMahon, A. P. (2000). A local Wnt-3a signal is required for development of the mammalian hippocampus. *Development*, 127(3), 457-467. Retrieved from <https://www.ncbi.nlm.nih.gov/pubmed/10631167>
- Li, G., Kataoka, H., Coughlin, S. R., & Pleasure, S. J. (2009). Identification of a transient subpial neurogenic zone in the developing dentate gyrus and its regulation by Cxcl12 and reelin signaling. *Development*, 136(2), 327-335. doi:10.1242/dev.025742
- Li, G., & Pleasure, S. J. (2014). The development of hippocampal cellular assemblies. *Wiley Interdiscip Rev Dev Biol*, 3(2), 165-177. doi:10.1002/wdev.127
- Lu, M., Grove, E. A., & Miller, R. J. (2002). Abnormal development of the hippocampal dentate gyrus in mice lacking the CXCR4 chemokine receptor. *Proceedings of the National Academy of Sciences of the United States of America*, 99(10), 7090-7095. doi:10.1073/pnas.092013799

1000 Mangale, V. S., Hirokawa, K. E., Satyaki, P. R., Gokulchandran, N., Chikbire, S., Subramanian, L., . . .
1001 Monuki, E. S. (2008). Lhx2 selector activity specifies cortical identity and suppresses
1002 hippocampal organizer fate. *Science*, 319(5861), 304-309. doi:10.1126/science.1151695
1003 Mariani, J., Favaro, R., Lancini, C., Vaccari, G., Ferri, A. L., Bertolini, J., . . . Nicolis, S. K. (2012). Emx2
1004 is a dose-dependent negative regulator of Sox2 telencephalic enhancers. *Nucleic acids*
1005 *research*, 40(14), 6461-6476. doi:10.1093/nar/gks295
1006 Mercurio, S., Serra, L., Motta, A., Gesuita, L., Sanchez-Arrones, L., Inverardi, F., . . . Nicolis, S. K.
1007 (2019). Sox2 Acts in Thalamic Neurons to Control the Development of Retina-Thalamus-
1008 Cortex Connectivity. *iScience*, 15, 257-273. doi:10.1016/j.isci.2019.04.030
1009 Meyer, G., Cabrera Socorro, A., Perez Garcia, C. G., Martinez Millan, L., Walker, N., & Caput, D.
1010 (2004). Developmental roles of p73 in Cajal-Retzius cells and cortical patterning. *The*
1011 *Journal of neuroscience : the official journal of the Society for Neuroscience*, 24(44), 9878-
1012 9887. doi:10.1523/JNEUROSCI.3060-04.2004
1013 Meyer, G., Gonzalez-Arnay, E., Moll, U., Nemajerova, A., Tissir, F., & Gonzalez-Gomez, M. (2019).
1014 Cajal-Retzius neurons are required for the development of the human hippocampal fissure.
1015 *J Anat*, 235(3), 569-589. doi:10.1111/joa.12947
1016 Meyer, G., Schaaps, J. P., Moreau, L., & Goffinet, A. M. (2000). Embryonic and early fetal
1017 development of the human neocortex. *The Journal of neuroscience : the official journal of*
1018 *the Society for Neuroscience*, 20(5), 1858-1868. Retrieved from
1019 <https://www.ncbi.nlm.nih.gov/pubmed/10684887>
1020 Miles, R., & Wong, R. K. (1983). Single neurones can initiate synchronized population discharge in
1021 the hippocampus. *Nature*, 306(5941), 371-373. doi:10.1038/306371a0
1022 Mimura-Yamamoto, Y., Shinohara, H., Kashiwagi, T., Sato, T., Shioda, S., & Seki, T. (2017).
1023 Dynamics and function of CXCR4 in formation of the granule cell layer during hippocampal
1024 development. *Sci Rep*, 7(1), 5647. doi:10.1038/s41598-017-05738-7
1025 Moser, M. B., & Moser, E. I. (1998). Functional differentiation in the hippocampus. *Hippocampus*,
1026 8(6), 608-619. doi:10.1002/(SICI)1098-1063(1998)8:6<608::AID-HIPO3>3.0.CO;2-7
1027 Muotri, A. R., Marchetto, M. C., Coufal, N. G., Oefner, R., Yeo, G., Nakashima, K., & Gage, F. H.
1028 (2010). L1 retrotransposition in neurons is modulated by MeCP2. *Nature*, 468(7322), 443-
1029 446. doi:10.1038/nature09544
1030 Naruse, I., Ueta, E., Sumino, Y., Ogawa, M., & Ishikiriya, S. (2010). Birth defects caused by
1031 mutations in human GLI3 and mouse Gli3 genes. *Congenit Anom (Kyoto)*, 50(1), 1-7.
1032 doi:10.1111/j.1741-4520.2009.00266.x
1033 Panaliappan, T. K., Wittmann, W., Jidigam, V. K., Mercurio, S., Bertolini, J. A., Sghari, S., . . .
1034 Gunhaga, L. (2018). Sox2 is required for olfactory pit formation and olfactory neurogenesis
1035 through BMP restriction and Hes5 upregulation. *Development*, 145(2).
1036 doi:10.1242/dev.153791
1037 Ragge, N. K., Lorenz, B., Schneider, A., Bushby, K., de Sanctis, L., de Sanctis, U., . . . Fitzpatrick, D. R.
1038 (2005). SOX2 anophthalmia syndrome. *Am J Med Genet A*, 135(1), 1-7.
1039 doi:10.1002/ajmg.a.30642
1040 Roelink, H. (2000). Hippocampus formation: an intriguing collaboration. *Current biology : CB*,
1041 10(7), R279-281. Retrieved from <http://www.ncbi.nlm.nih.gov/pubmed/10753739>
1042 Rogers, N., Cheah, P. S., Szarek, E., Banerjee, K., Schwartz, J., & Thomas, P. (2013). Expression of
1043 the murine transcription factor SOX3 during embryonic and adult neurogenesis. *Gene Expr*
1044 *Patterns*, 13(7), 240-248. doi:10.1016/j.gep.2013.04.004

1045 Sisodiya, S. M., Ragge, N. K., Cavalleri, G. L., Hever, A., Lorenz, B., Schneider, A., . . . Fitzpatrick, D.
1046 R. (2006). Role of SOX2 mutations in human hippocampal malformations and epilepsy.
1047 *Epilepsia*, 47(3), 534-542. doi:10.1111/j.1528-1167.2006.00464.x
1048 Srinivas, S., Watanabe, T., Lin, C. S., William, C. M., Tanabe, Y., Jessell, T. M., & Costantini, F.
1049 (2001). Cre reporter strains produced by targeted insertion of EYFP and ECFP into the
1050 ROSA26 locus. *BMC developmental biology*, 1, 4. doi:10.1186/1471-213x-1-4
1051 Swanson, L. W., & Cowan, W. M. (1977). An autoradiographic study of the organization of the
1052 efferent connections of the hippocampal formation in the rat. *The Journal of comparative*
1053 *neurology*, 172(1), 49-84. doi:10.1002/cne.901720104
1054 Theil, T., Alvarez-Bolado, G., Walter, A., & Ruther, U. (1999). Gli3 is required for Emx gene
1055 expression during dorsal telencephalon development. *Development*, 126(16), 3561-3571.
1056 Retrieved from <https://www.ncbi.nlm.nih.gov/pubmed/10409502>
1057 Theil, T., Aydin, S., Koch, S., Grotewold, L., & Ruther, U. (2002). Wnt and Bmp signalling
1058 cooperatively regulate graded Emx2 expression in the dorsal telencephalon. *Development*,
1059 129(13), 3045-3054. Retrieved from <https://www.ncbi.nlm.nih.gov/pubmed/12070081>
1060 Traub, R. D., Jefferys, J. G. R., & Whittington, M. A. (1999). *Fast oscillations in cortical circuits*.
1061 Cambridge, Mass.: MIT Press.
1062 Tronche, F., Kellendonk, C., Kretz, O., Gass, P., Anlag, K., Orban, P. C., . . . Schutz, G. (1999).
1063 Disruption of the glucocorticoid receptor gene in the nervous system results in reduced
1064 anxiety. *Nature genetics*, 23(1), 99-103. doi:10.1038/12703
1065 Venkatesan, K., Liu, Y., & Goldfarb, M. (2014). Fast-onset long-term open-state block of sodium
1066 channels by A-type FHF mediates classical spike accommodation in hippocampal
1067 pyramidal neurons. *The Journal of neuroscience : the official journal of the Society for*
1068 *Neuroscience*, 34(48), 16126-16139. doi:10.1523/JNEUROSCI.1271-14.2014
1069 Visel, A., Blow, M. J., Li, Z., Zhang, T., Akiyama, J. A., Holt, A., . . . Pennacchio, L. A. (2009). ChIP-seq
1070 accurately predicts tissue-specific activity of enhancers. *Nature*, 457(7231), 854-858.
1071 doi:10.1038/nature07730
1072 Wei, C. L., Nicolis, S. K., Zhu, Y., & Pagin, M. (2019). Sox2-Dependent 3D Chromatin Interactomes
1073 in Transcription, Neural Stem Cell Proliferation and Neurodevelopmental Diseases. *J Exp*
1074 *Neurosci*, 13, 1179069519868224. doi:10.1177/1179069519868224
1075 Witter, M. P., & Amaral, D. G. (2004). Hippocampal formation. In E. Paxinos (Ed.), *The Rat Nervous*
1076 *System* (third ed., pp. 635-704): Elsevier.
1077 Yang, A., Walker, N., Bronson, R., Kaghad, M., Oosterwegel, M., Bonnin, J., . . . Caput, D. (2000).
1078 p73-deficient mice have neurological, pheromonal and inflammatory defects but lack
1079 spontaneous tumours. *Nature*, 404(6773), 99-103. doi:10.1038/35003607
1080 Zhong, S., Ding, W., Sun, L., Lu, Y., Dong, H., Fan, X., . . . Wang, X. (2020). Decoding the
1081 development of the human hippocampus. *Nature*, 577(7791), 531-536.
1082 doi:10.1038/s41586-019-1917-5
1083